

Supplementary Information

Selective Inhibition of Bacterial Topoisomerase I by alkynyl- bisbenzimidazoles

Nihar Ranjan^a, Geraldine Fulcrand^b, Ada King^c, Joseph Brown^d, Xiuping Jiang^d, Fenfei Leng^b
and Dev P. Arya^{a,c*}

^aDepartment of Chemistry, Clemson University, Clemson, South Carolina, Unite States 29634

^b Department of Chemistry and Biochemistry, Florida International University, Miami, Florida 33199 (Unite States)

^cNUBAD, LLC, 900 B West Faris Road, Greenville, South Carolina 29605

^d Department of Biological Sciences, Clemson University, Clemson, South Carolina 29634

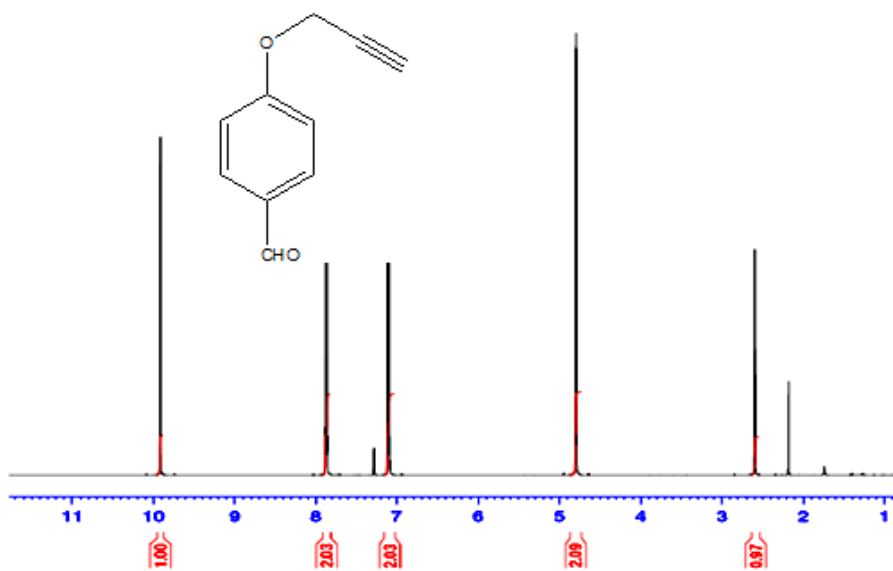


Figure S1a. ^1H NMR spectrum of DPA151-a.

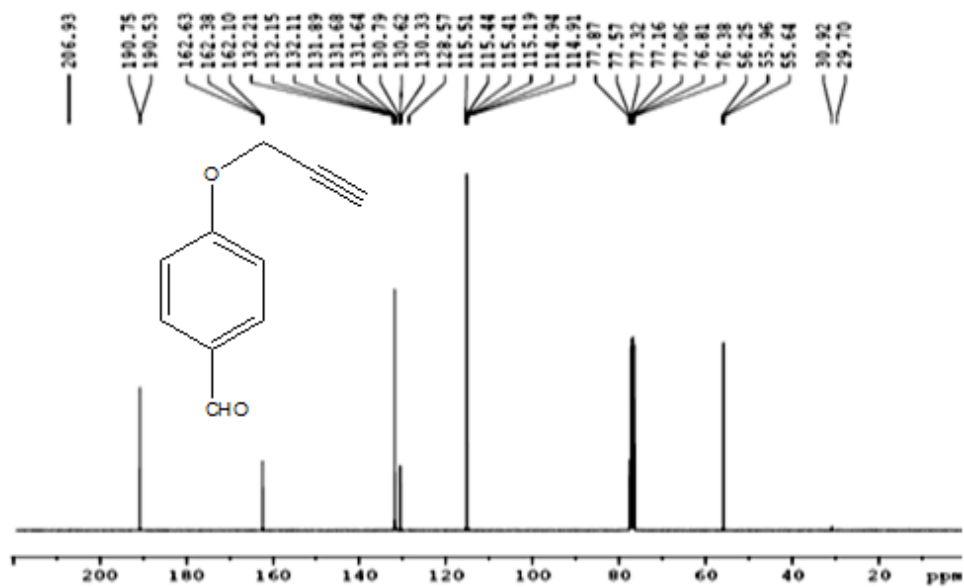


Figure S1b. ^{13}C NMR spectrum of DPA151-a.

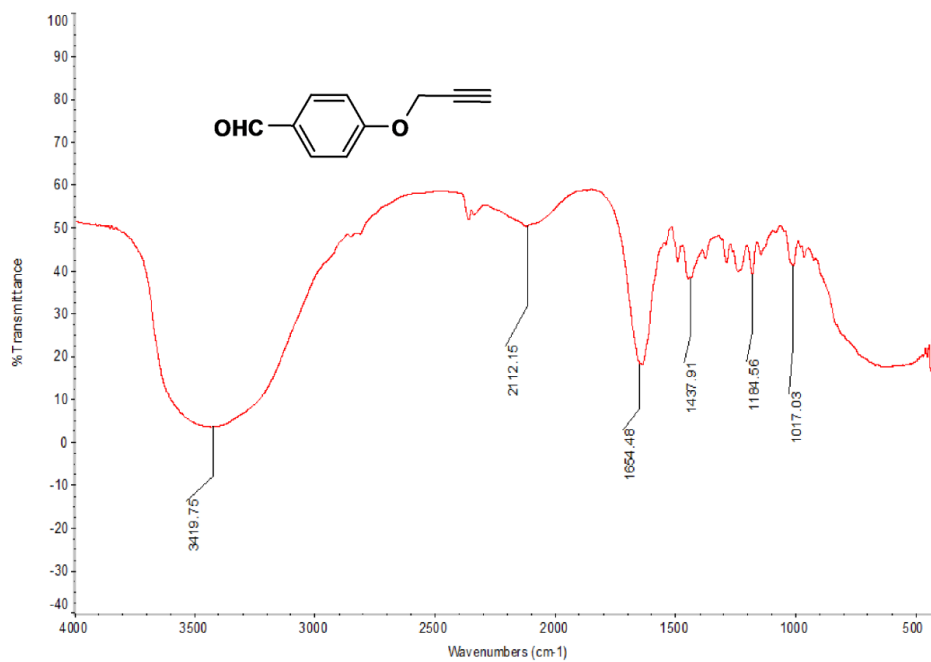


Figure S1c. IR spectrum of DPA151-a..

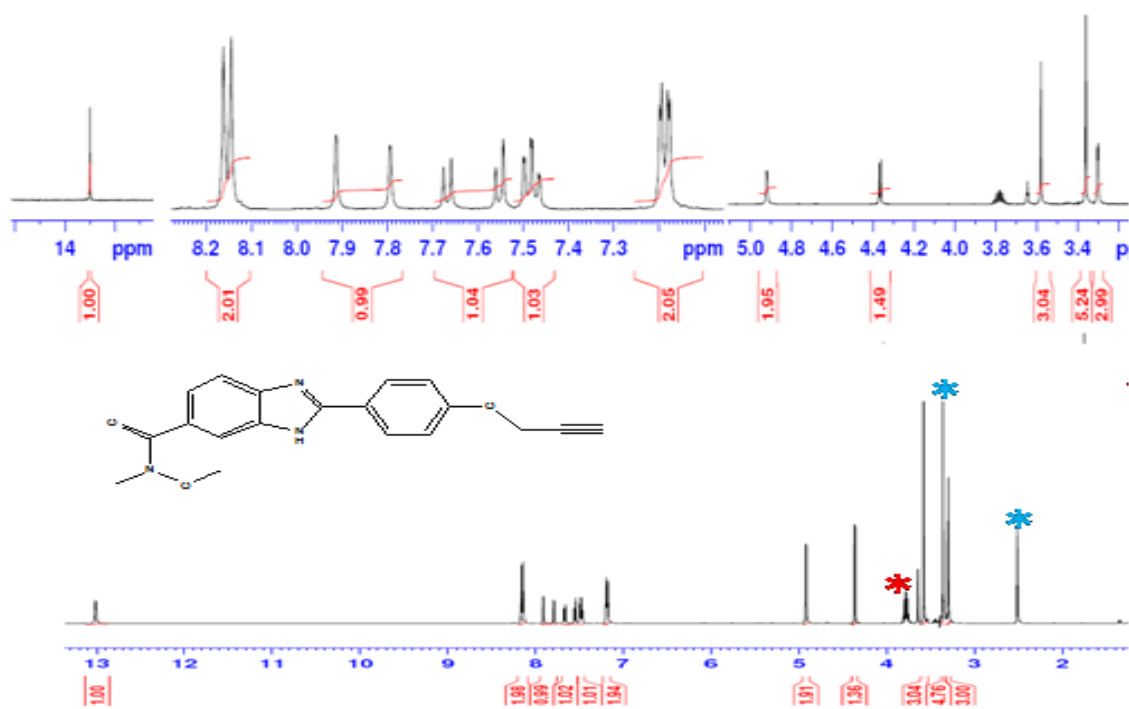


Figure S2a. ¹H NMR spectrum of DPA151-b (Stars indicate solvent peaks).

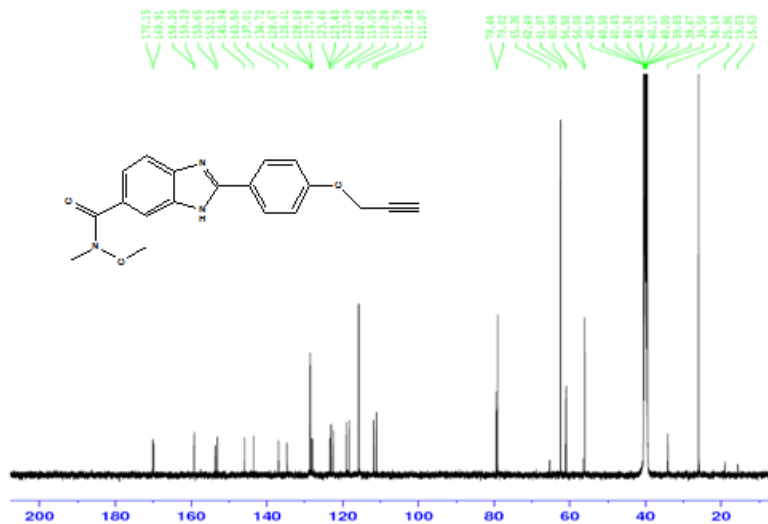


Figure S2b. ¹³C NMR spectrum of DPA151-b.

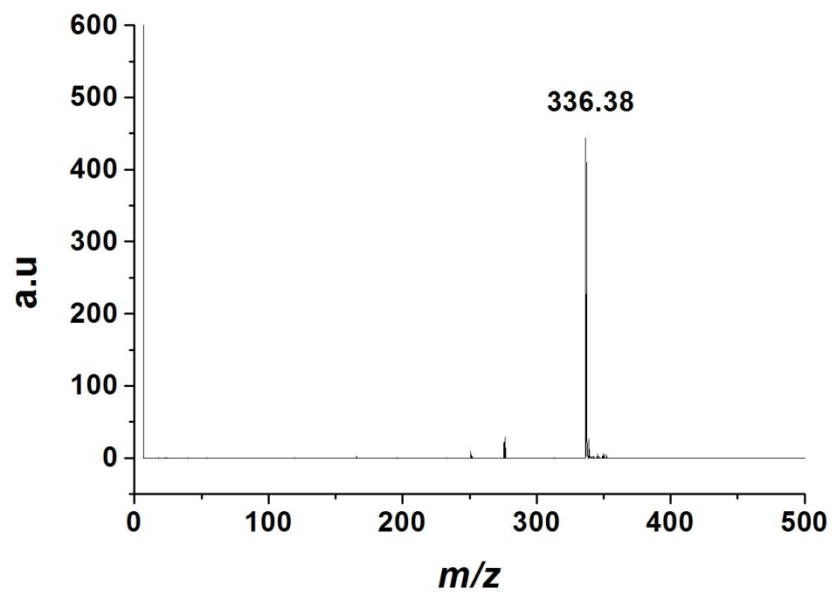


Figure S2c. MALDI-TOF spectrum of DPA151-b.

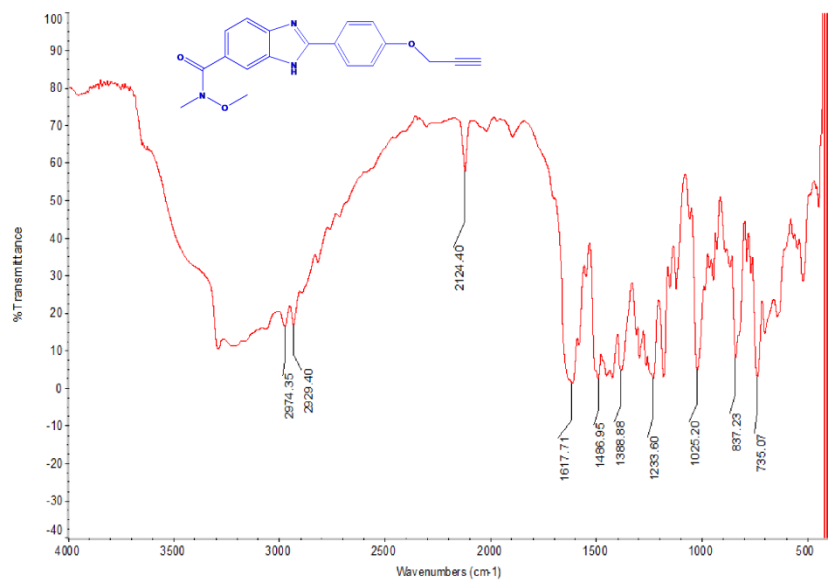


Figure S2d. IR spectrum of DPA151-b.

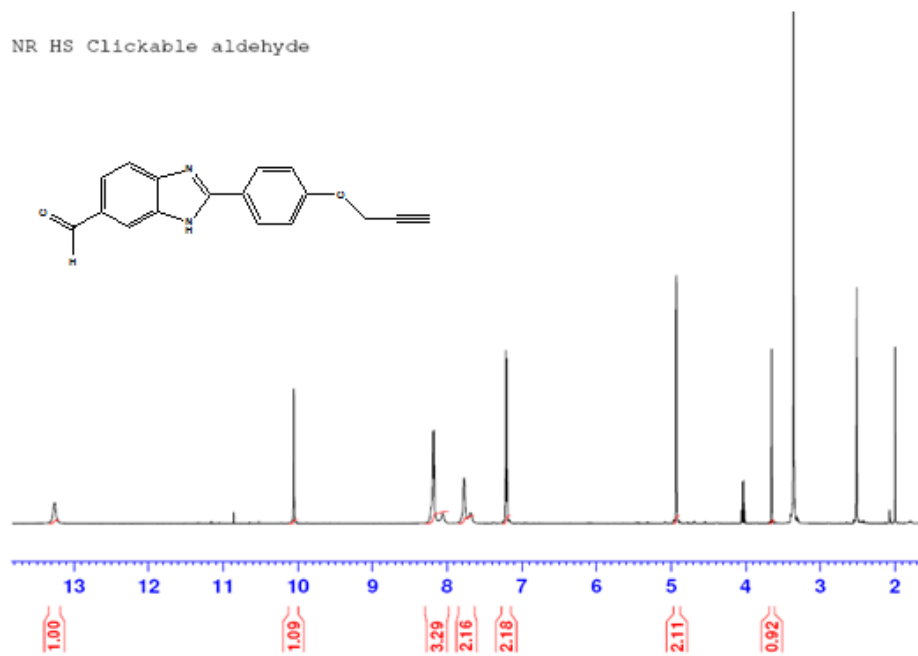


Figure S3a. ^1H NMR spectrum of DPA151-c.

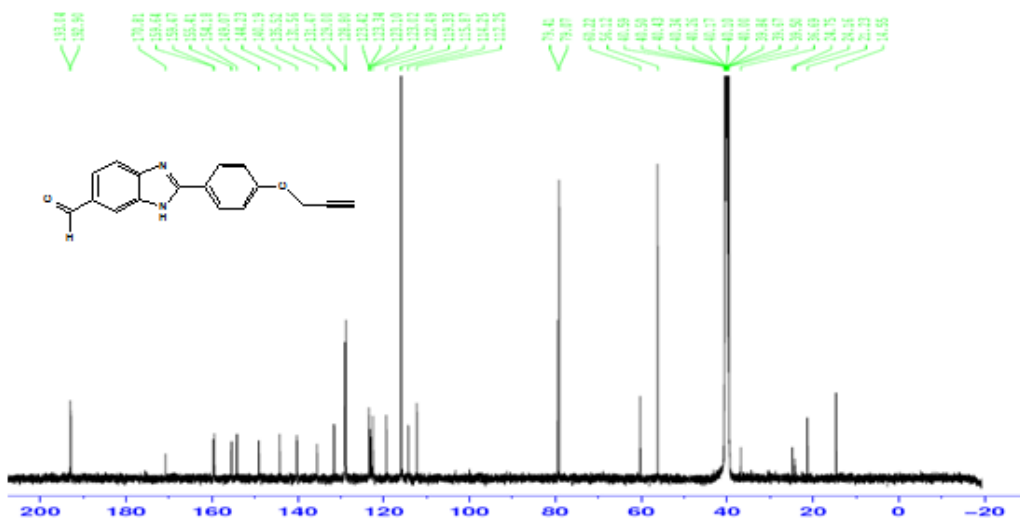


Figure S3b. ¹³C NMR spectrum of DPA151-c.

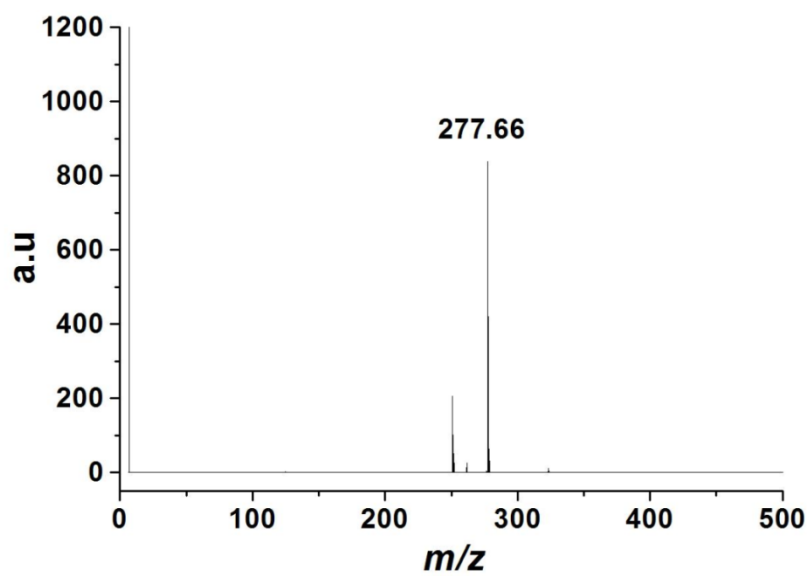


Figure S3c. MALDI-TOF spectrum of DPA151-c.

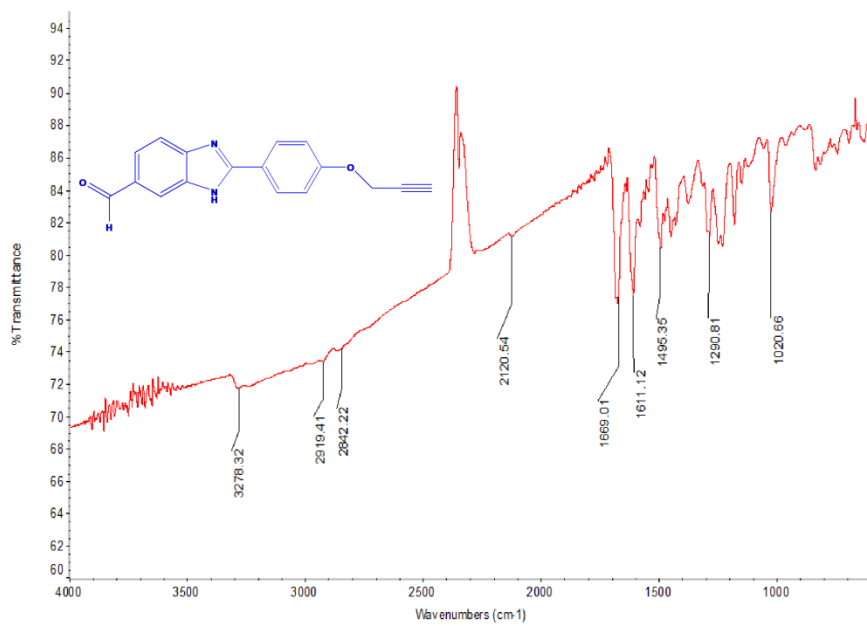


Figure S3d. IR spectrum of DPA151-c.

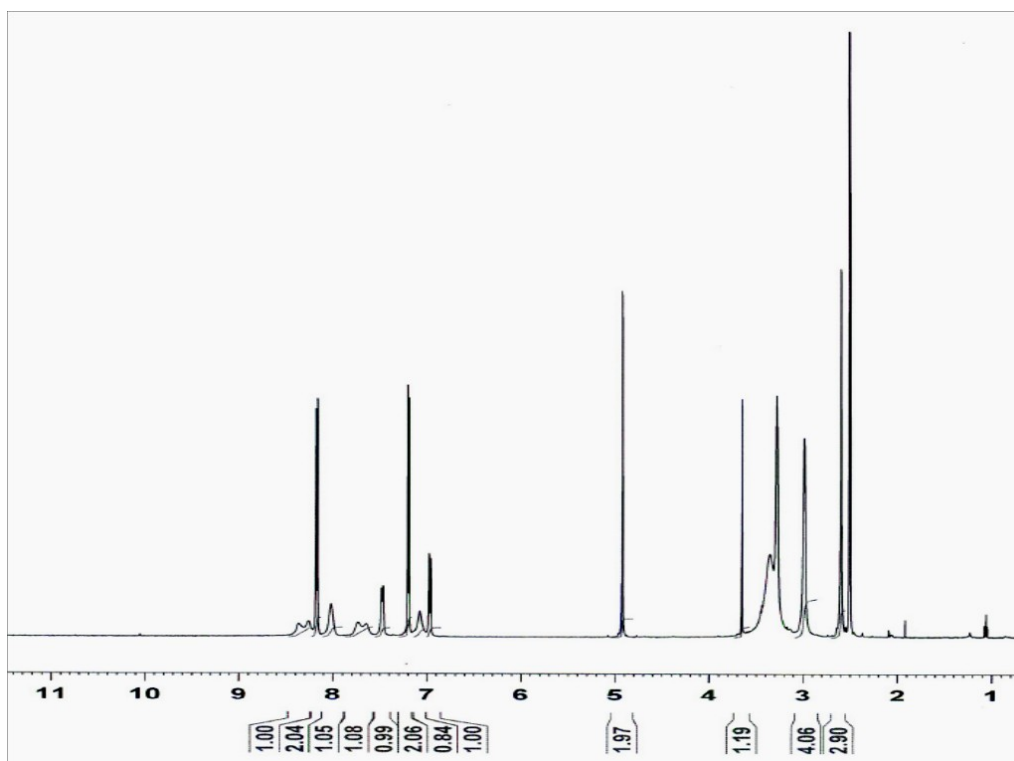


Figure S4a. ^1H NMR spectrum of DPA 151.

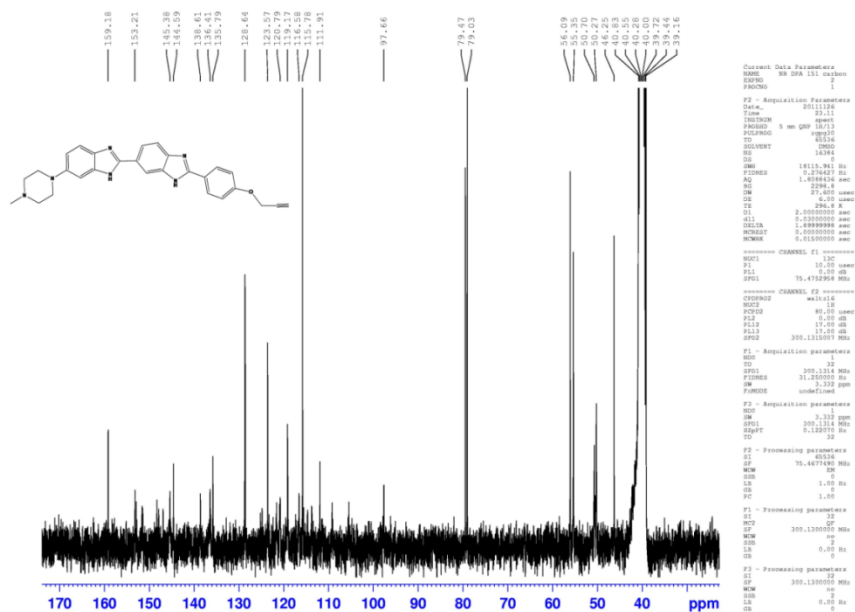


Figure S4b. ^{13}C NMR spectrum of DPA 151.

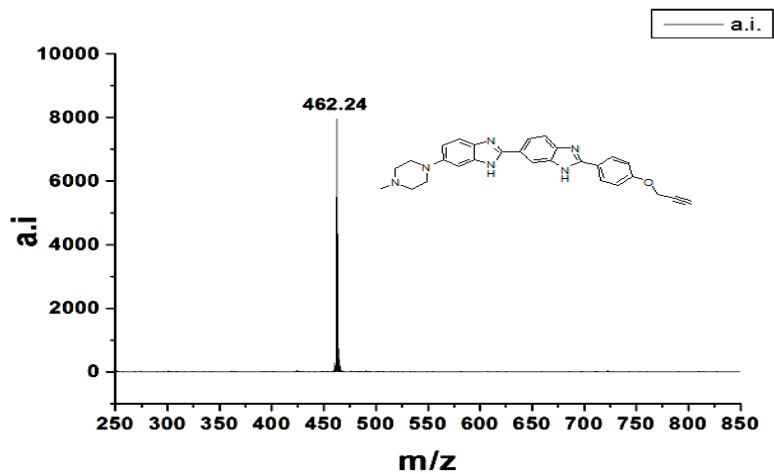


Figure S4c. MALDI-TOF spectrum of DPA 151.

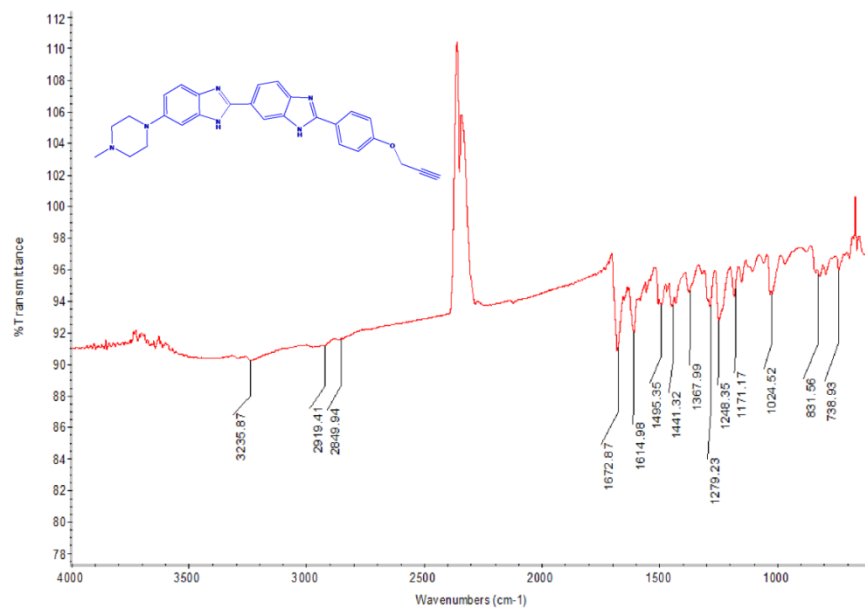


Figure S4d. IR spectrum of DPA 151.

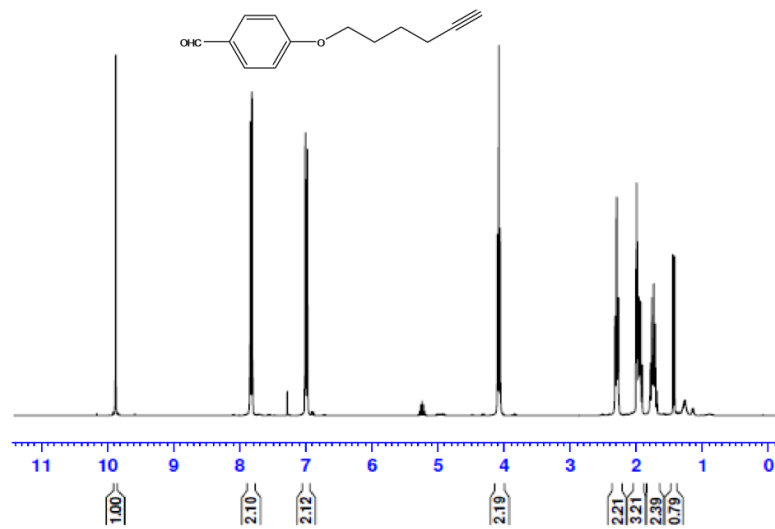


Figure S5a. ¹H NMR spectrum of DPA 152-a.

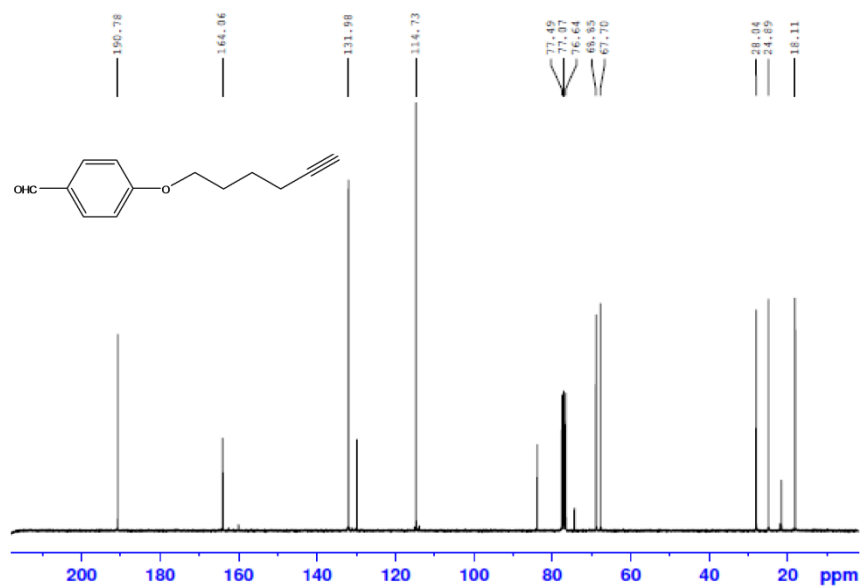


Figure S5b. ¹³C NMR spectrum of DPA 152-a.

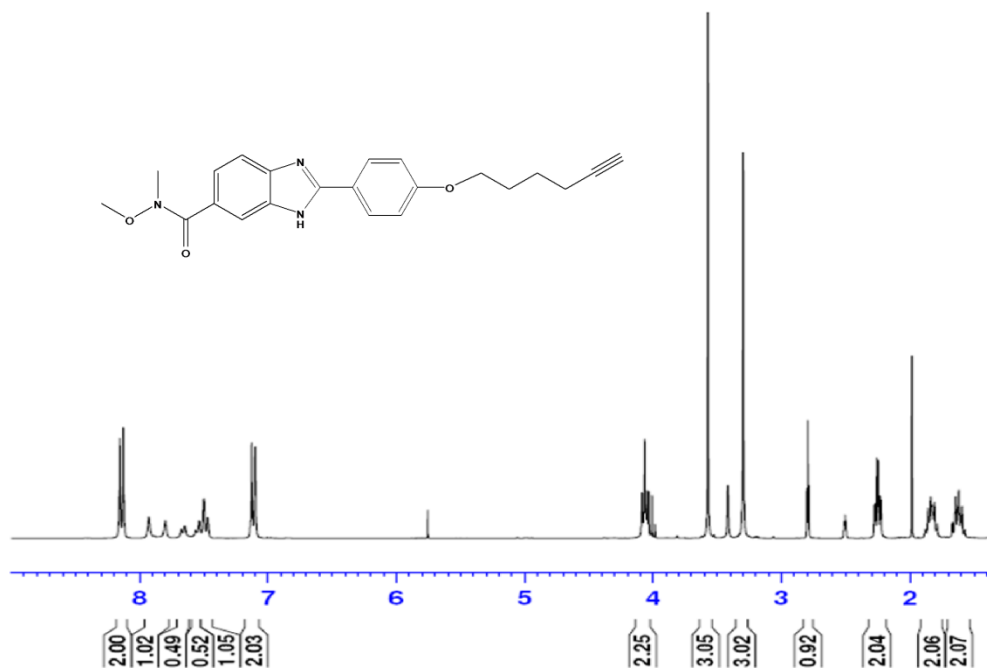


Figure S6a. ¹H NMR spectrum of DPA 152-b.

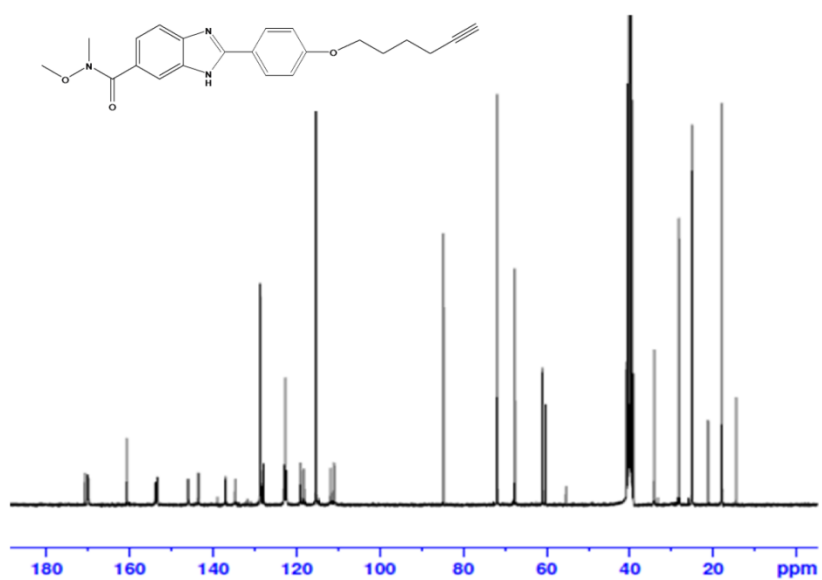


Figure S6b. ¹³C NMR spectrum of DPA 152-b.

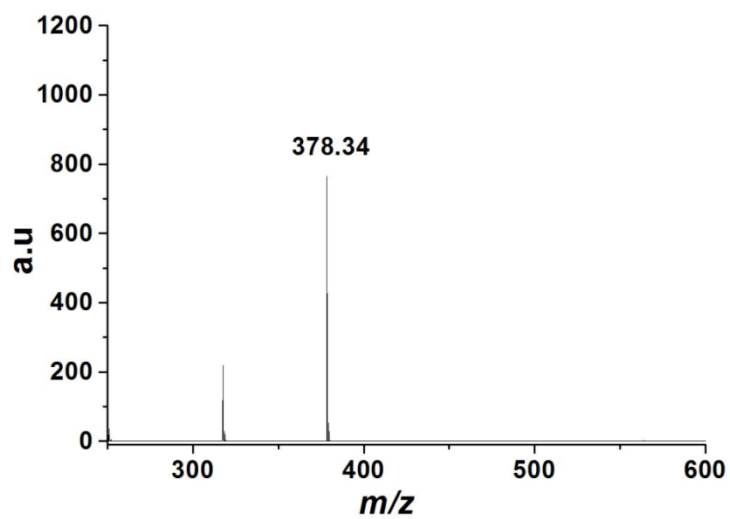


Figure S6c. MALDI-TOF spectrum of DPA 152-b.

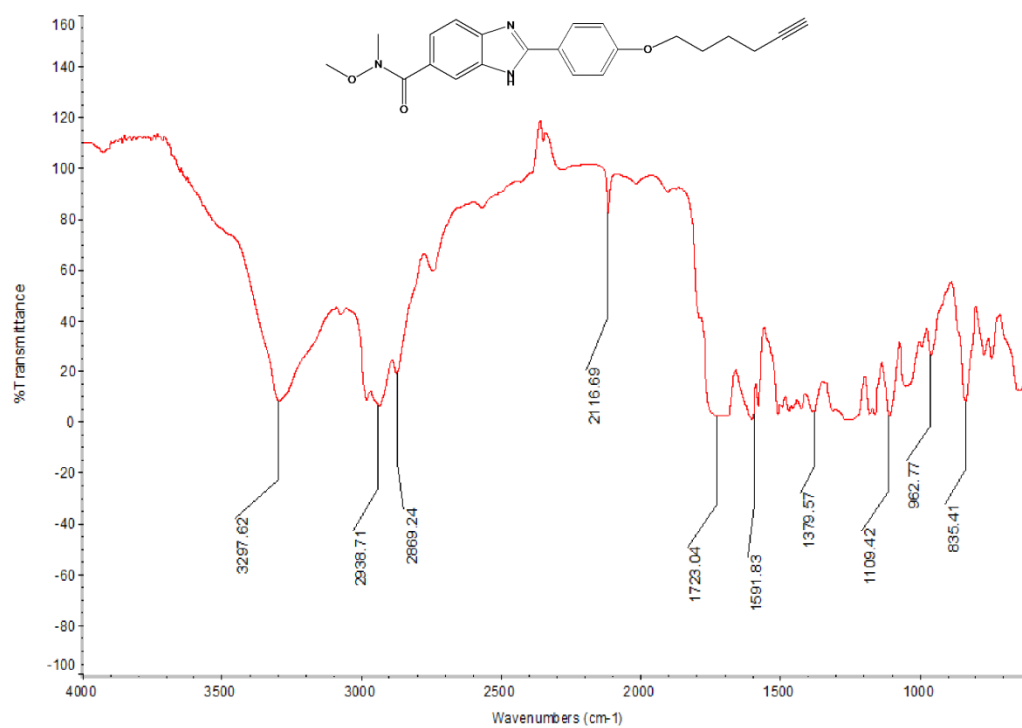


Figure S6d. IR spectrum of DPA 152-b.

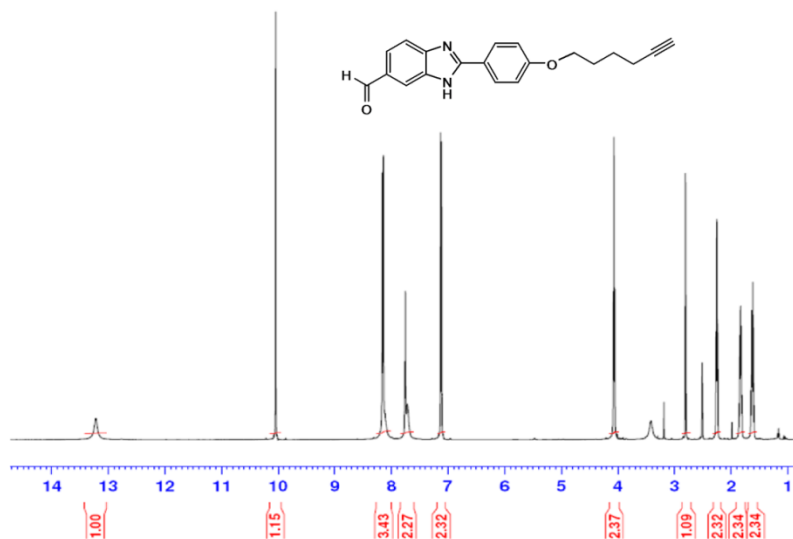


Figure S7a. ¹H NMR spectrum of compound DPA 152-c.

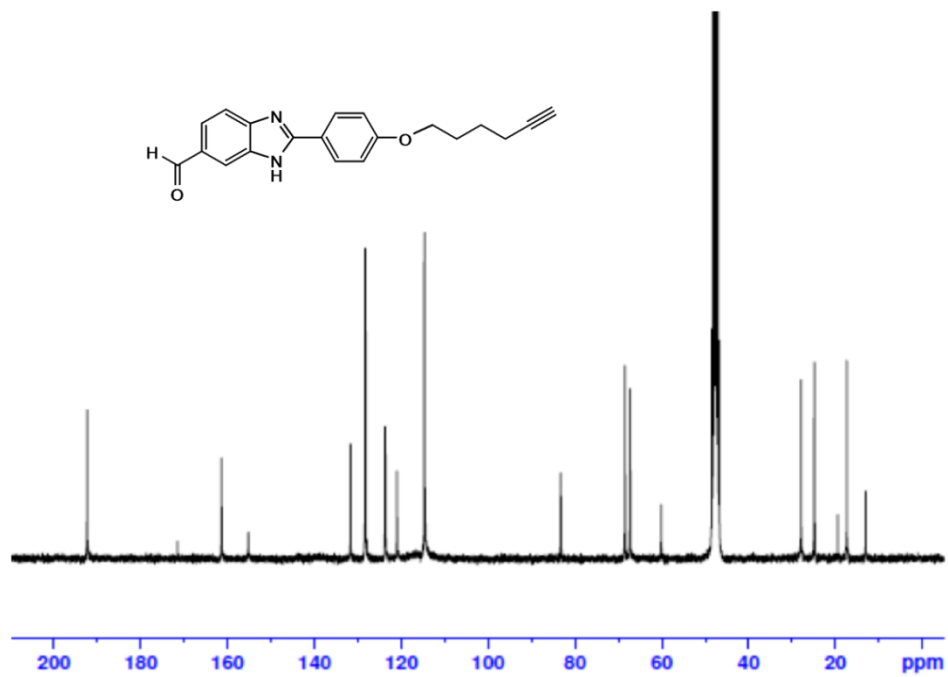


Figure S7b. ¹³C NMR spectrum of DPA 152-c.

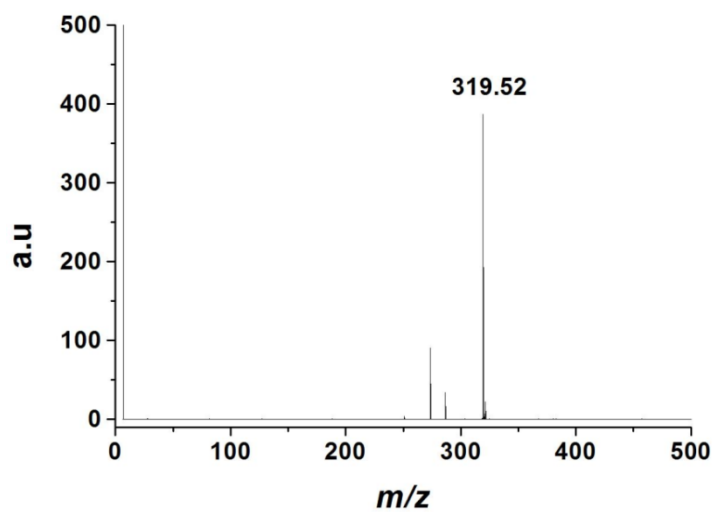


Figure S7c. MALDI-TOF spectrum of DPA 152-c.

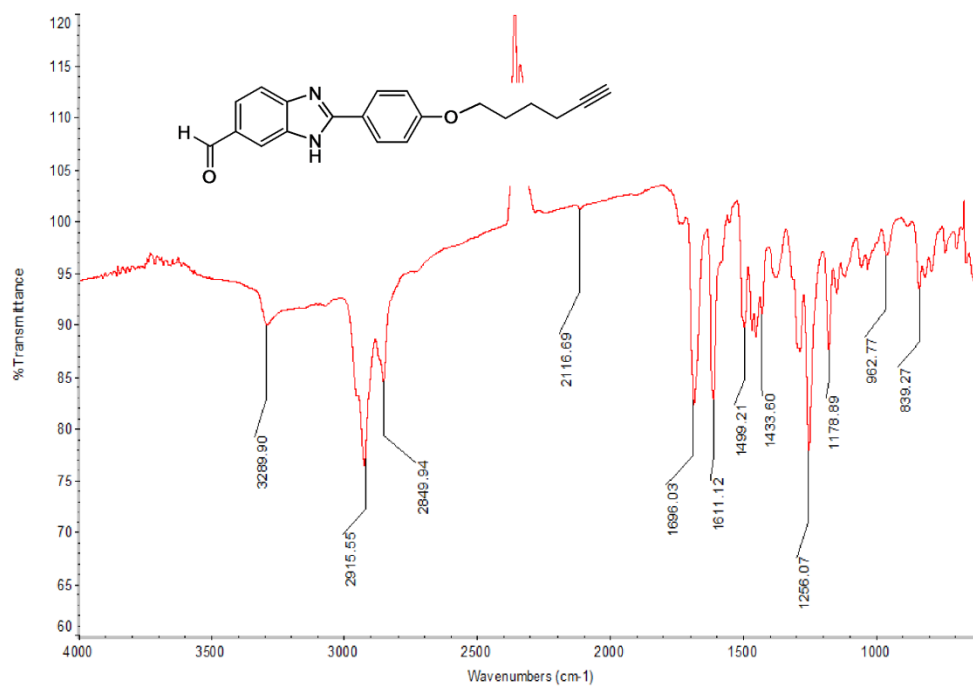


Figure S7d. IR spectrum of DPA 152-c.

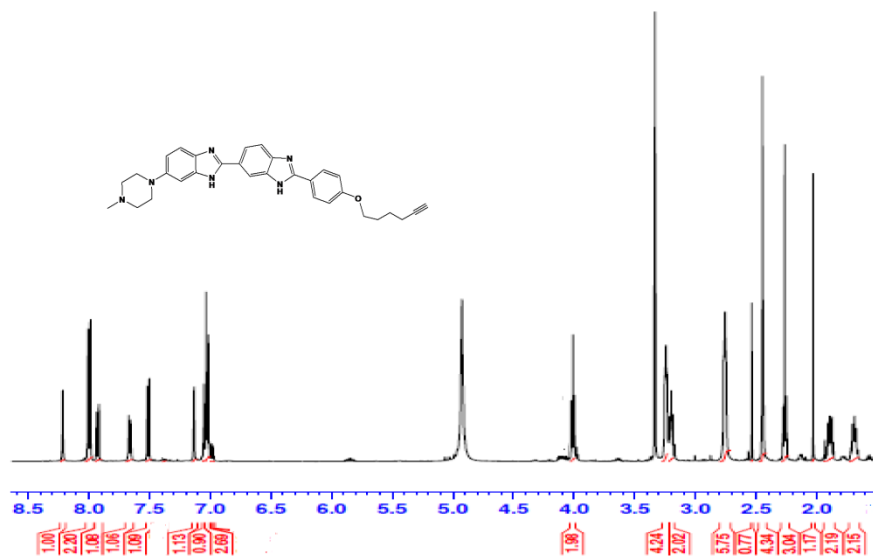


Figure S8a. ^1H NMR spectrum of DPA 152.

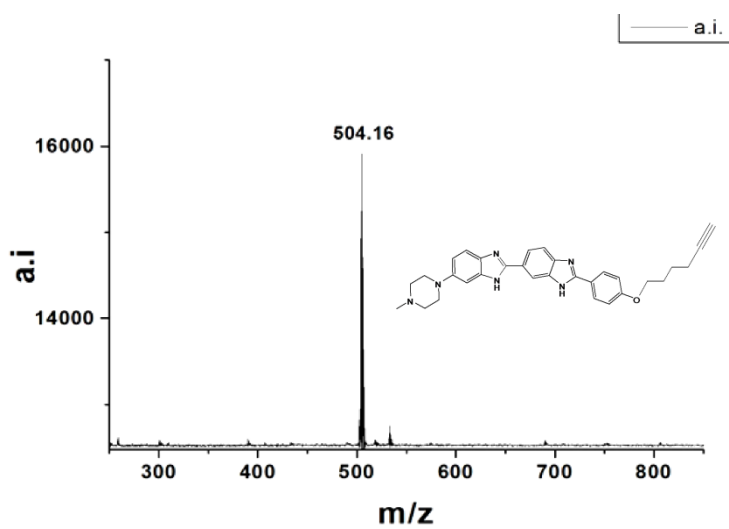


Figure S8b. MALDI-TOF spectrum of DPA 152.

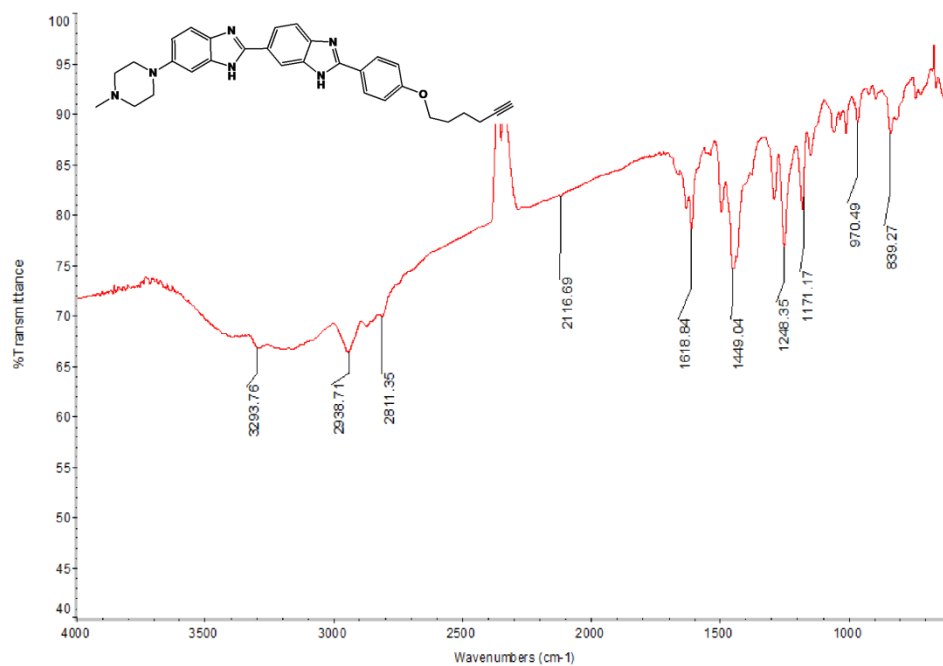


Figure S8c. IR spectrum of DPA 152.

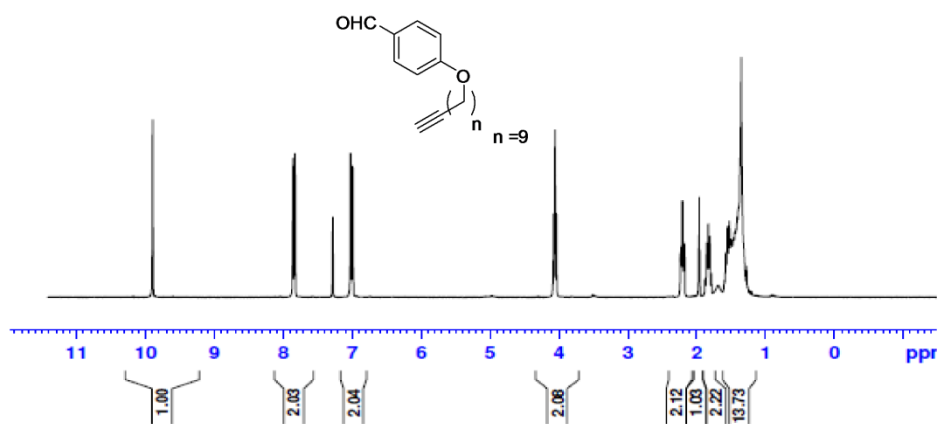


Figure S9a. ¹H NMR spectrum of DPA 153-a.

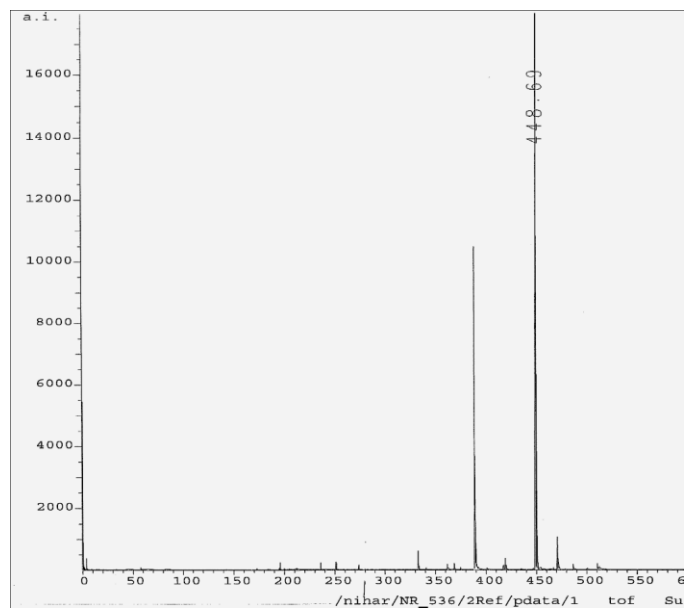


Figure S10c.MALDI-TOF spectrum of DPA 153-b.

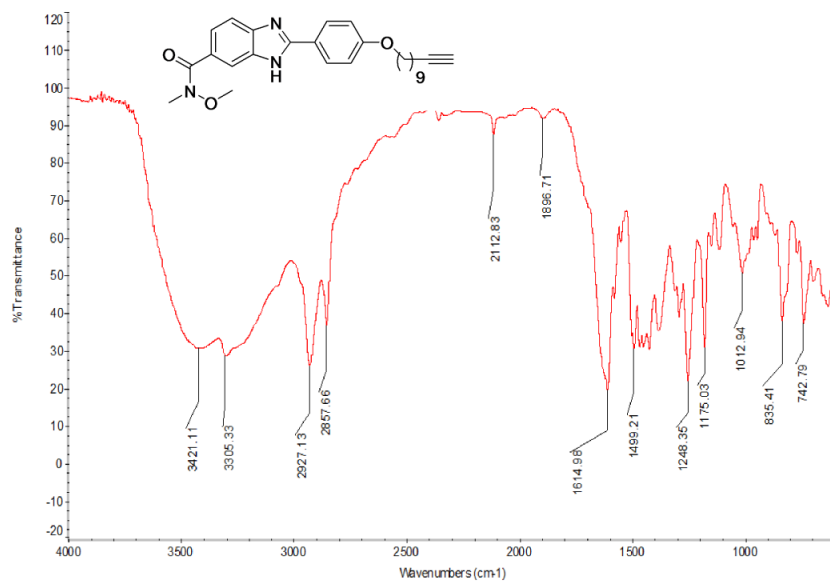


Figure S10d.IR spectrum of DPA 153-b.

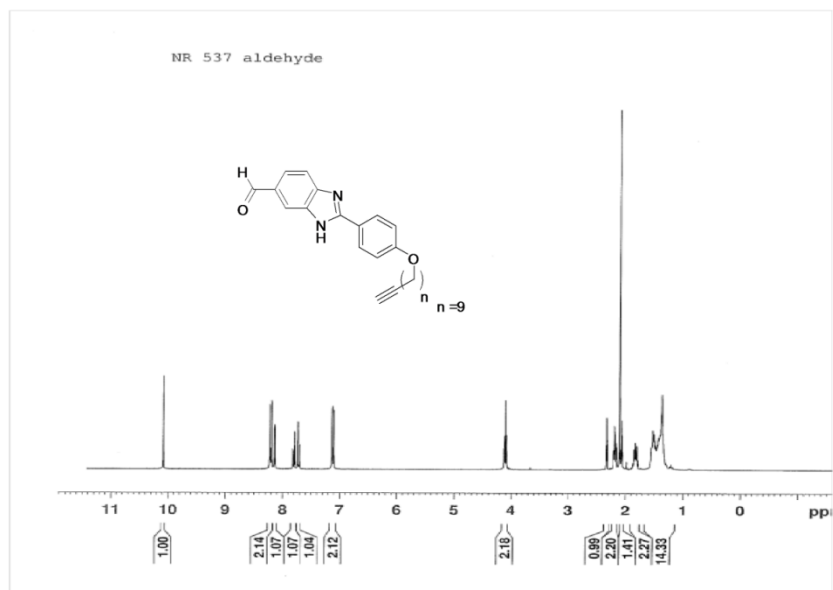


Figure S11a. ¹H NMR spectrum of DPA 153-c.

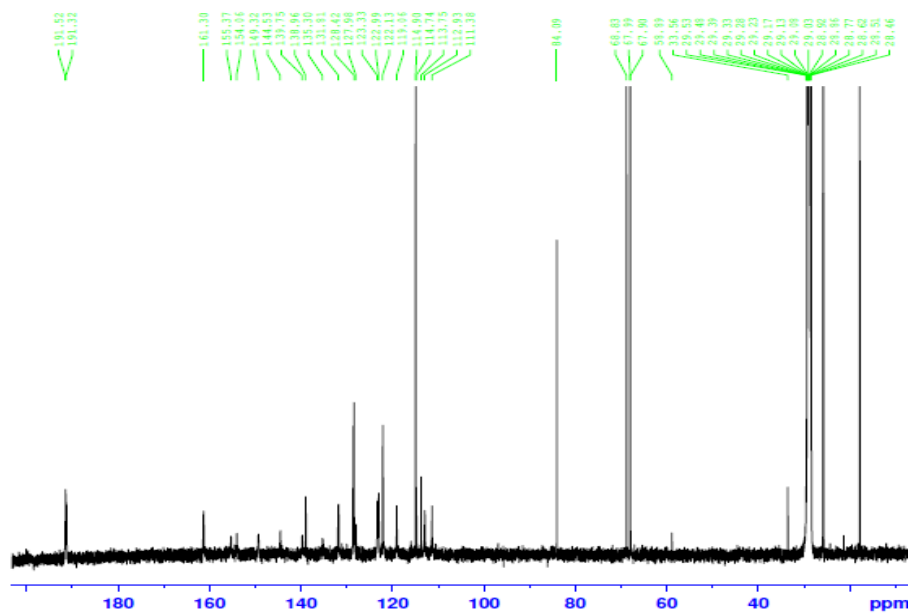


Figure S11b. ¹³C NMR spectrum of DPA 153-c.

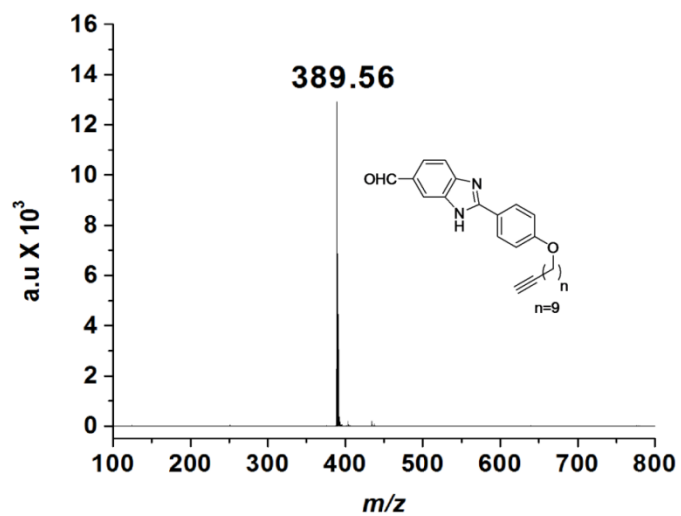


Figure S11c. MALDI-TOF spectrum of DPA 153-c.

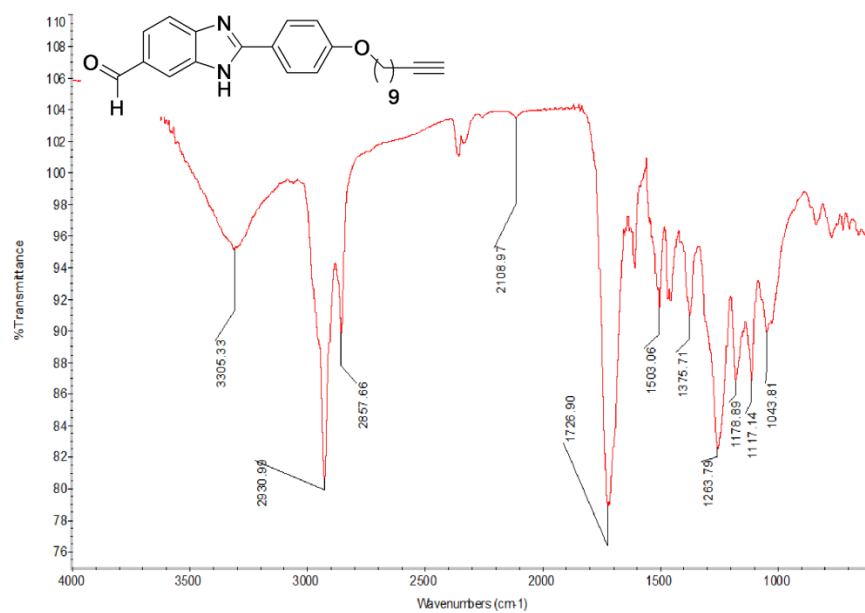


Figure S11d. IR spectrum of DPA 153-c.

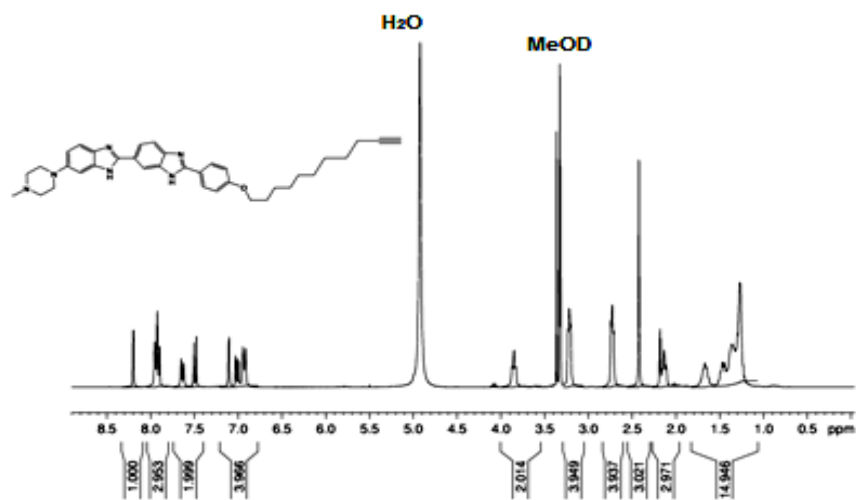


Figure S12a. ¹H NMR spectrum of DPA 153.

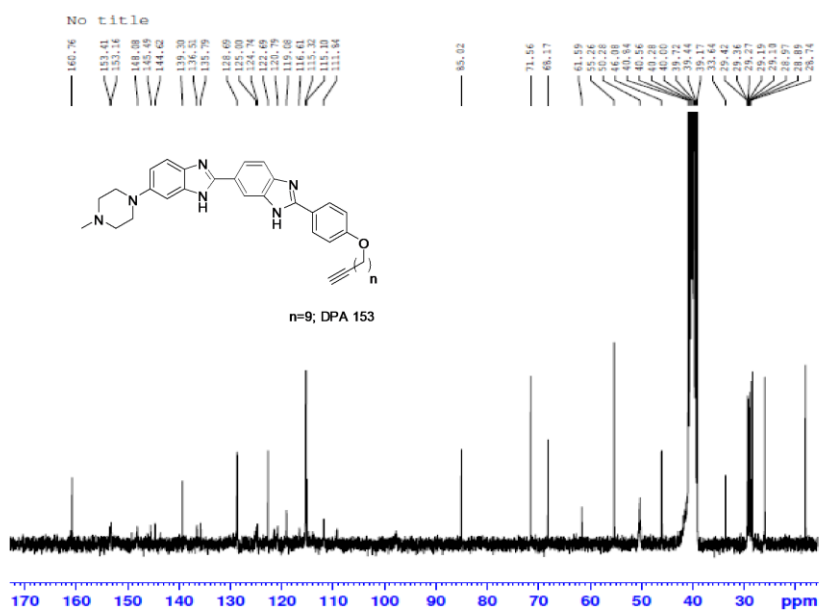


Figure S12b. ¹³C NMR spectrum of DPA 153.

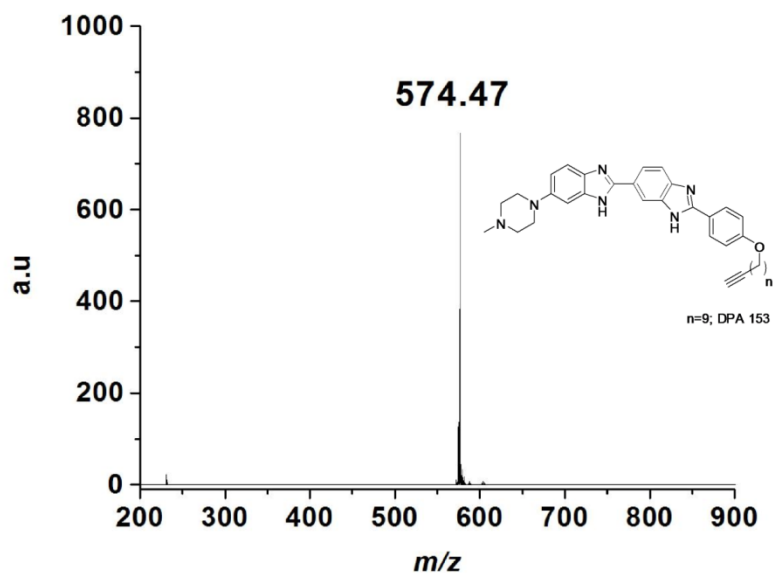


Figure S12c. MALDI-TOF spectrum of DPA 153.

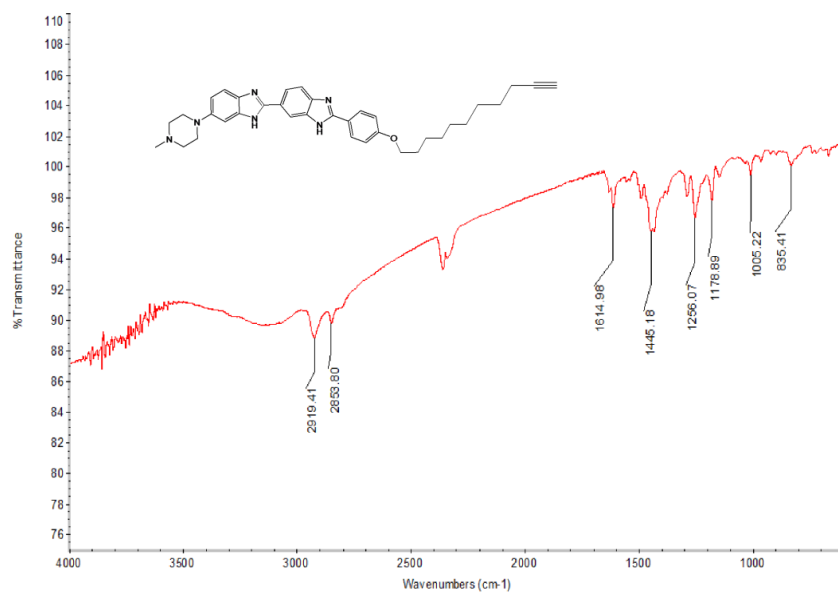


Figure S12d. IR spectrum of DPA 153.

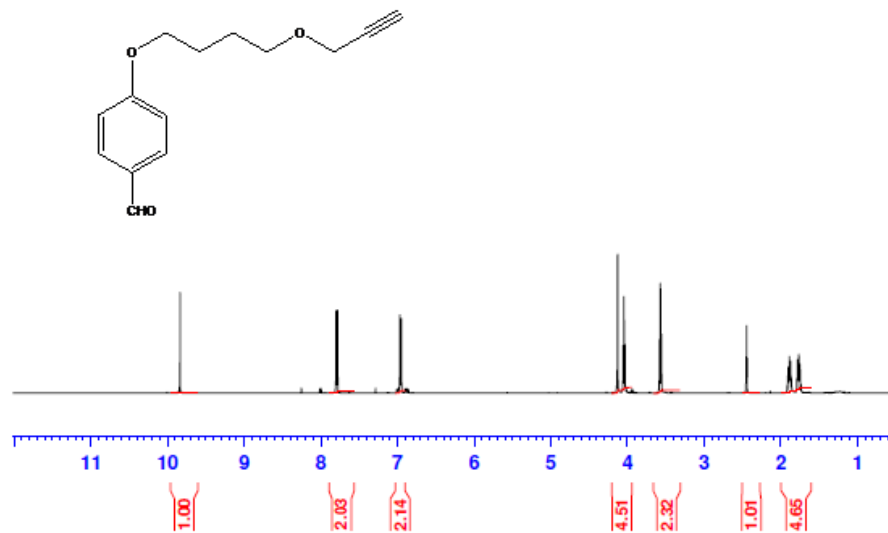


Figure S13a. ¹H NMR spectrum of DPA 154-a.

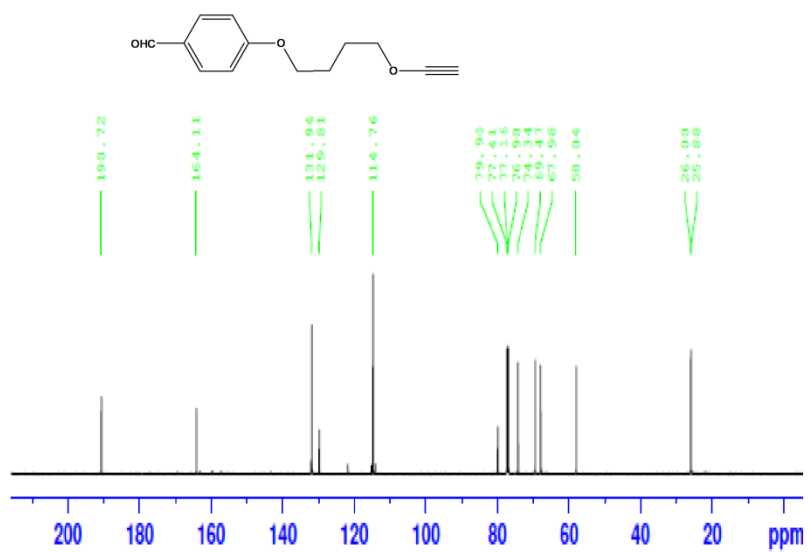


Figure S13b. ¹³C NMR spectrum of DPA 154-a.

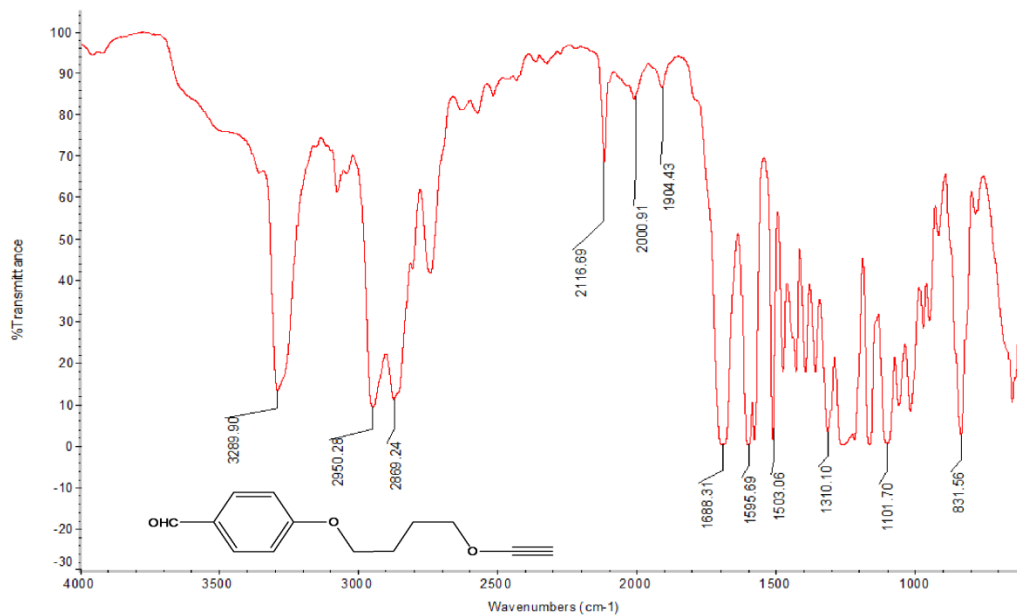


Figure S13c. IR spectrum of DPA 154-a.

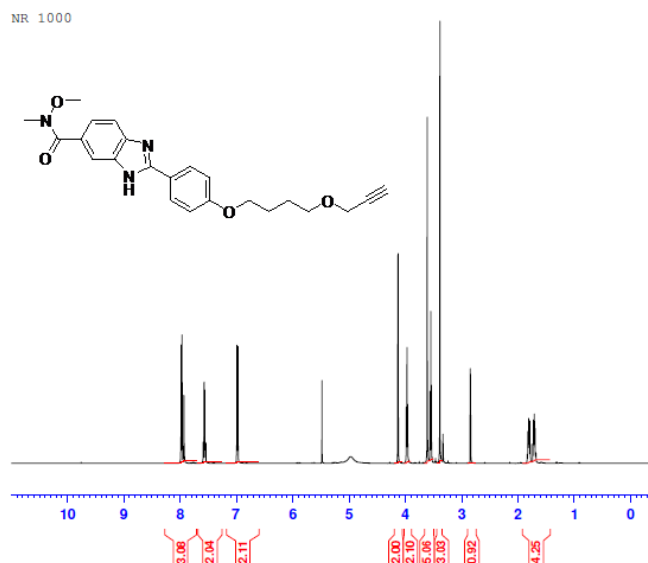


Figure S14a. ¹H NMR spectrum of DPA 154-b.

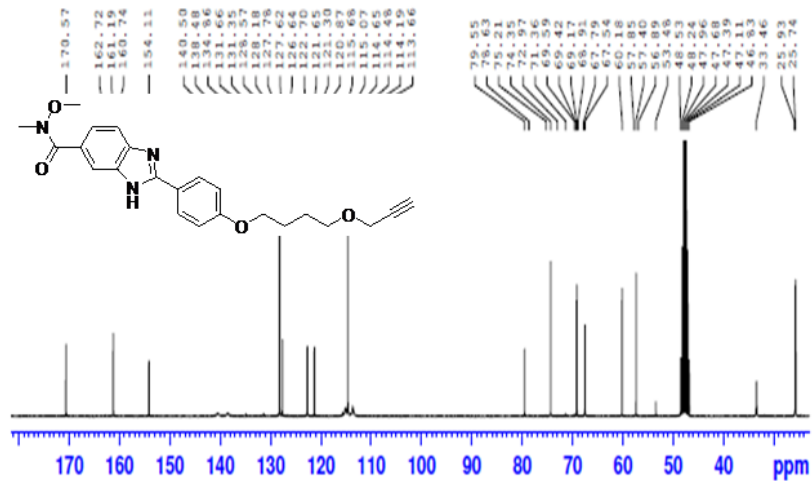


Figure S14b. ¹³C NMR spectrum of DPA 154-b.

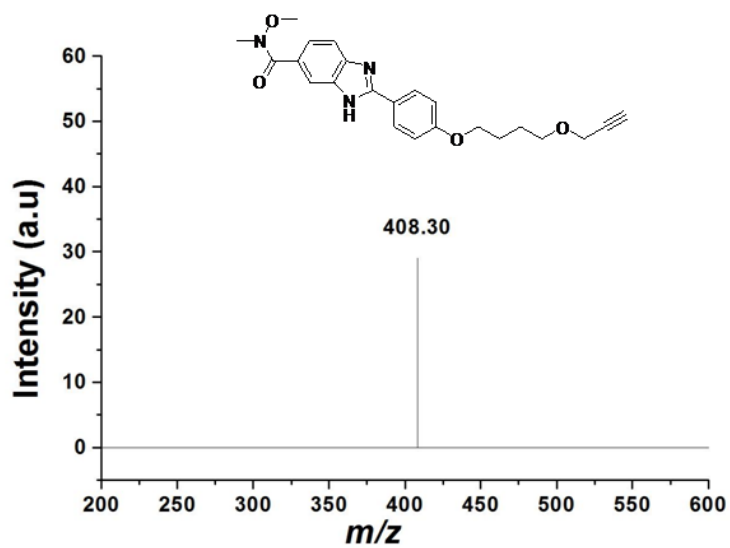


Figure S14c. MALDI-TOF spectrum of DPA 154-b.

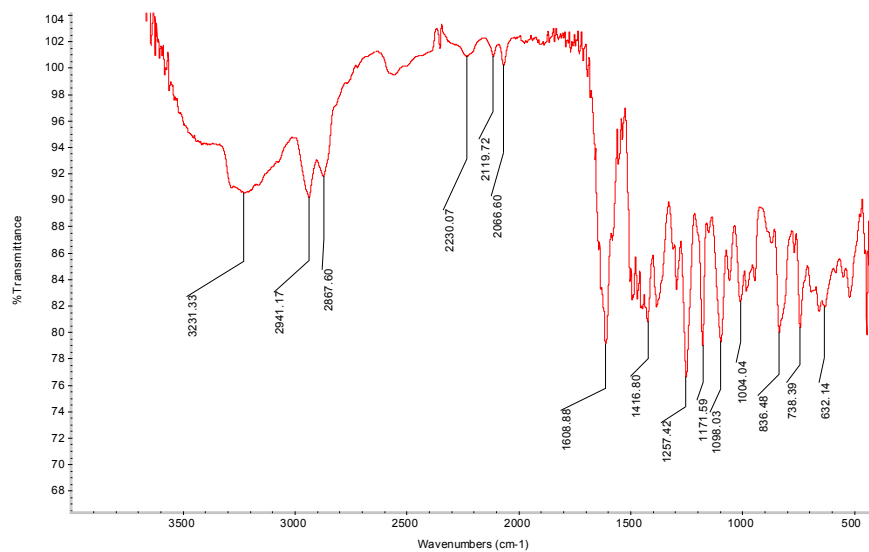


Figure S14d. IR spectrum of DPA 154-b.

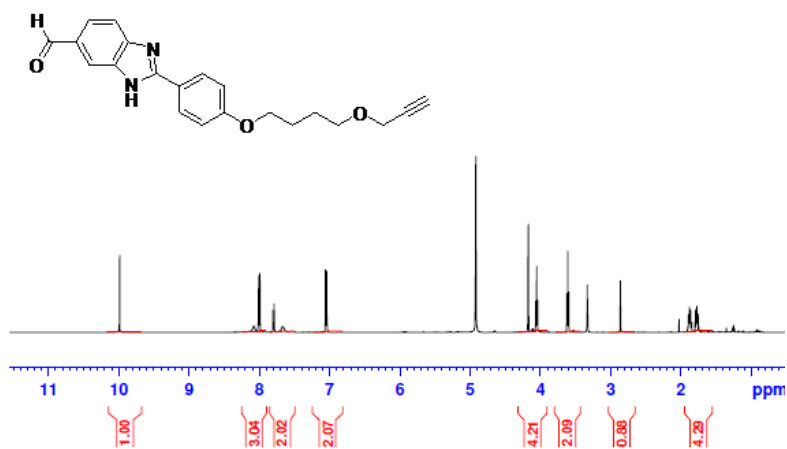


Figure S15a. ¹H NMR spectrum of DPA 154-c.

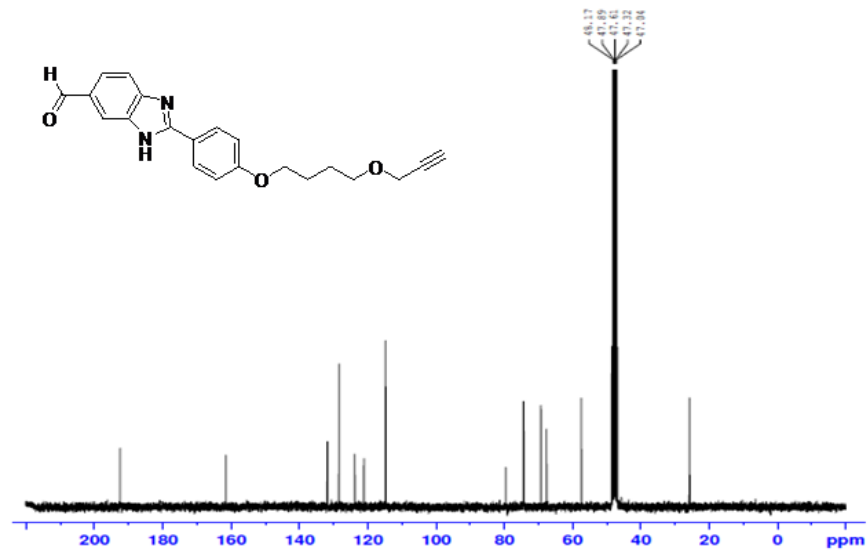


Figure S15b. ¹³C NMR spectrum of DPA 154-c.

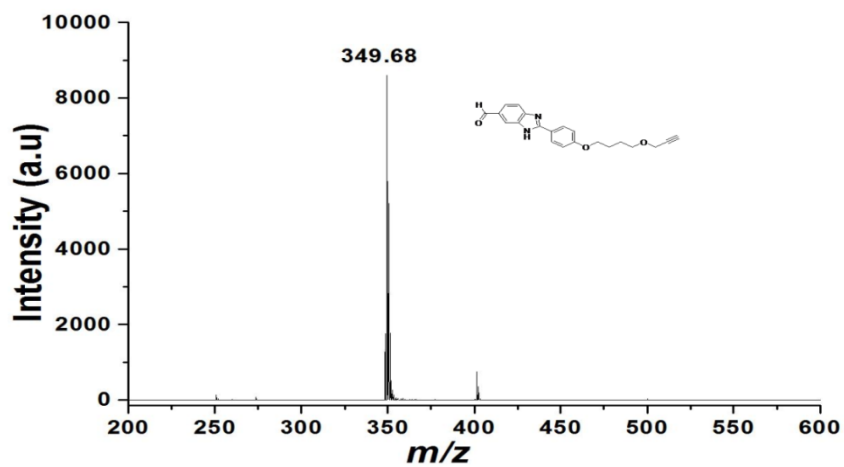


Figure S15c. MALDI-TOF spectrum of DPA 154-c.

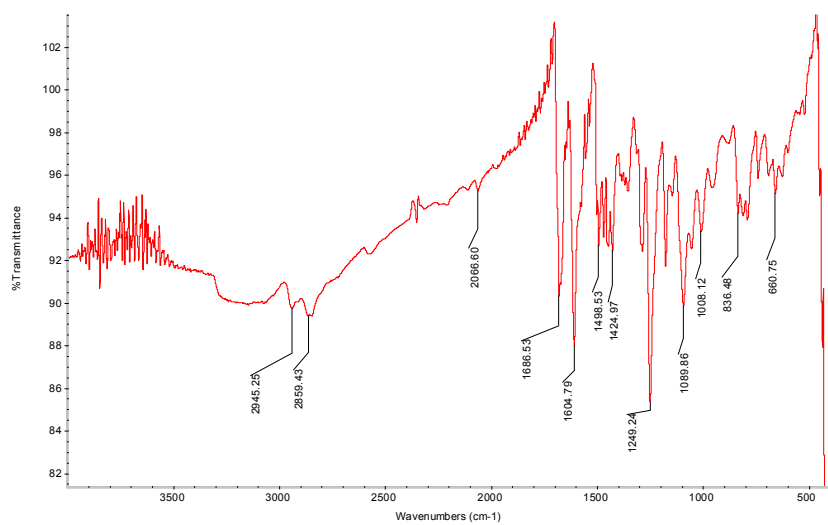


Figure S15d. IR spectrum of DPA 154-c.

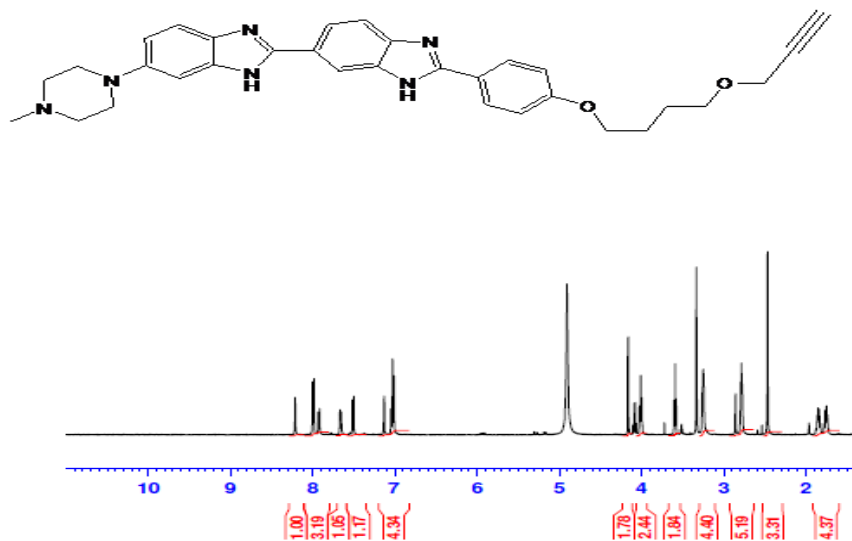


Figure S16a. ¹H NMR spectrum of DPA 154.

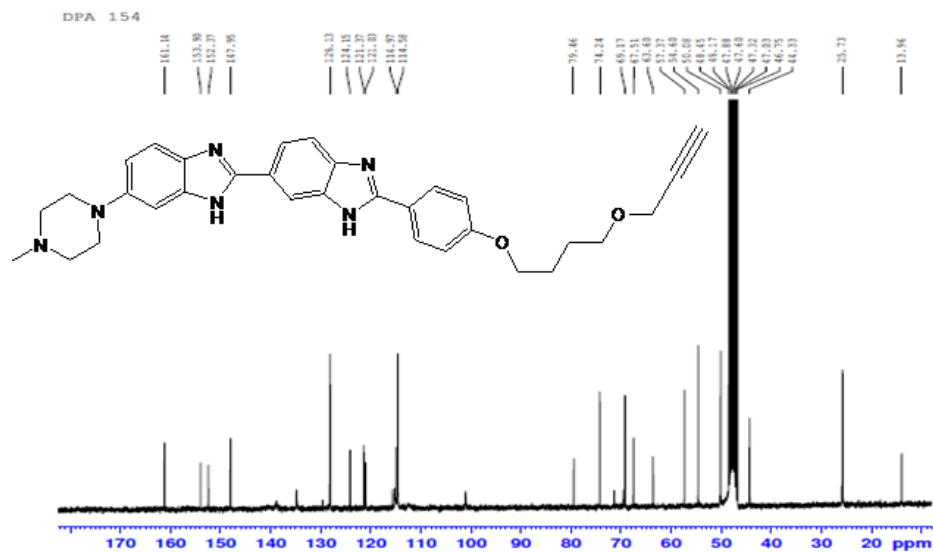


Figure S16b. ^{13}C NMR spectrum of DPA 154.

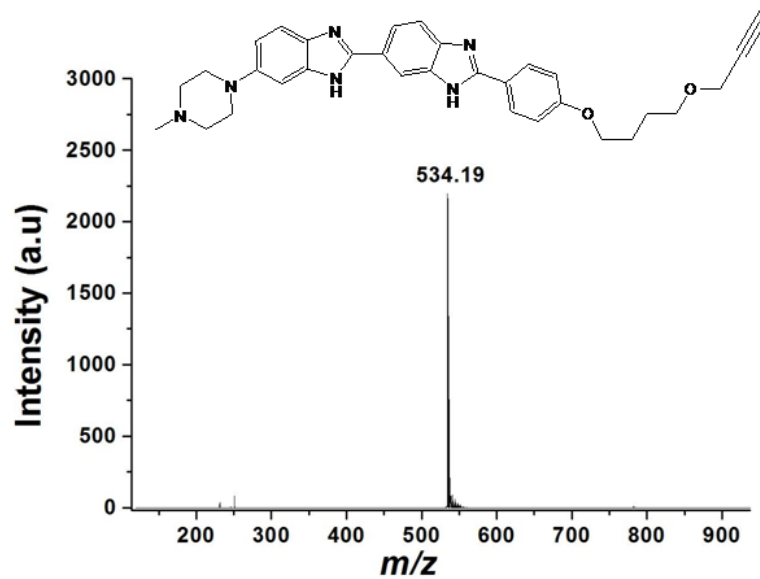


Figure S16c. MALDI-TOF spectrum of DPA 154.

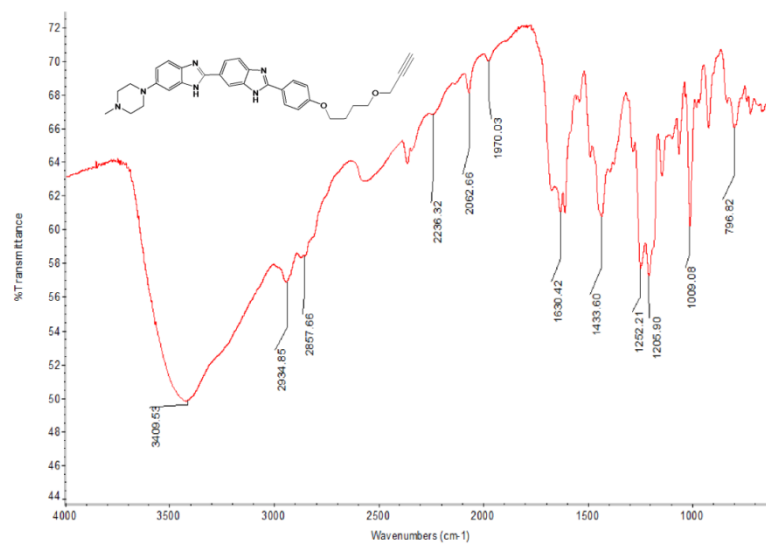


Figure S16d. IR spectrum of DPA 154.

Topoisomerase I inhibition results.

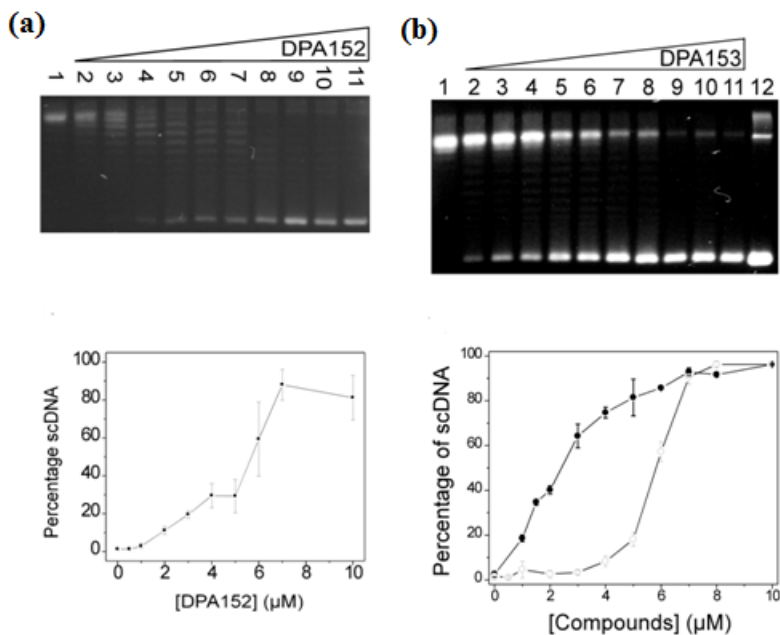


Figure S17. Inhibitory activities of compounds (a) DPA152 and (b) DPA153 against *E. coli* DNA topoisomerase I. The *E. coli* DNA topoisomerase I inhibition assays were performed as described in Materials and Methods. The plasmid DNA molecules were isolated and subjected to 1% agarose gel electrophoresis in the absence of chloroquine. (a) Lanes 1 to 11 contain 0, 0.5, 1.0, 2.0, 3.0, 4.0, 5.0, 6.0, 7.0, 8.0, and 10.0 μM of DPA152, respectively. The bottom panel shows the quantification analysis of the inhibitory activities of DPA152. (b) Lanes 1 to 11 contain 0, 1.0, 1.5, 2.0, 3.0, 4.0, 5.0, 6.0, 7.0, 8.0, and 10 μM of DPA153, respectively. Lane 12 is the supercoiled plasmid DNA pBAD-GFPuv. The bottom panel shows the quantification analysis of the inhibitory activities of DPA153.

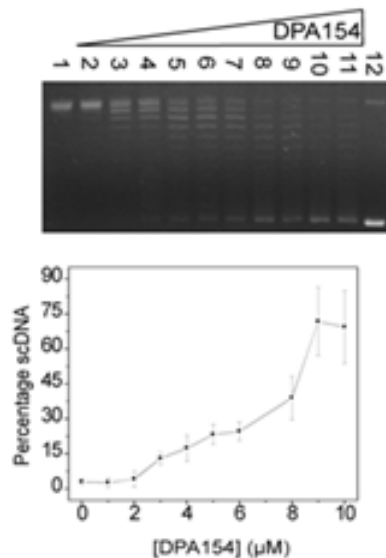


Figure S18. Inhibitory activities of compounds DPA154 against *E. coli* DNA topoisomerase I. The *E. coli* DNA topoisomerase I inhibition assays were performed as described in Materials and Methods. The plasmid DNA molecules were isolated and subjected to 1% agarose gel electrophoresis in the absence of chloroquine. Lanes 1 to 11 contain 0, 1.0, 2.0, 3.0, 4.0, 5.0, 6.0, 7.0, 8.0, 9.0, and 10.0 μM of DPA154, respectively. Lane 12 is the supercoiled plasmid DNA pBAD-GFPuv. The bottom panel shows the quantification analysis of the inhibitory activities of DPA154.

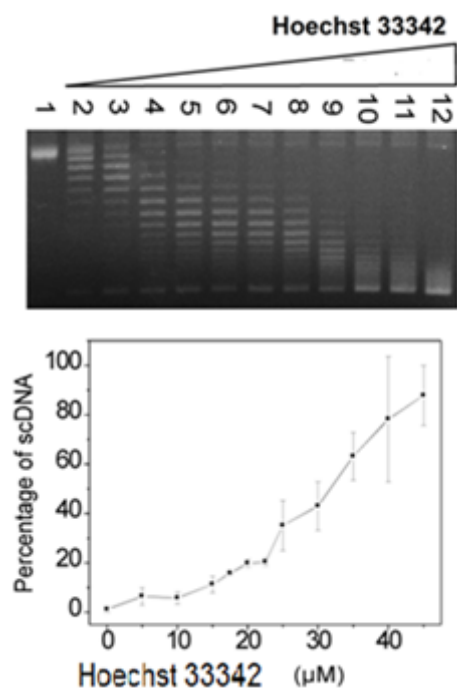


Figure S19. Inhibitory activities of compounds Hoechst 33342 and against *E. coli* DNA topoisomerase I. The *E. coli* DNA topoisomerase I inhibition assays were performed as described in Materials and Methods. The plasmid DNA molecules were isolated and subjected to 1% agarose gel electrophoresis in the absence of chloroquine. Lanes 1 to 12 contain 0, 5.0, 10.0, 15.0, 17.5, 20.0, 22.5, 25.0, 30.0, 35.0, 40.0, and 45.0 μM of Hoechst 33342, respectively. The bottom panel shows the quantification analysis of the inhibitory activities of Hoechst 33342.

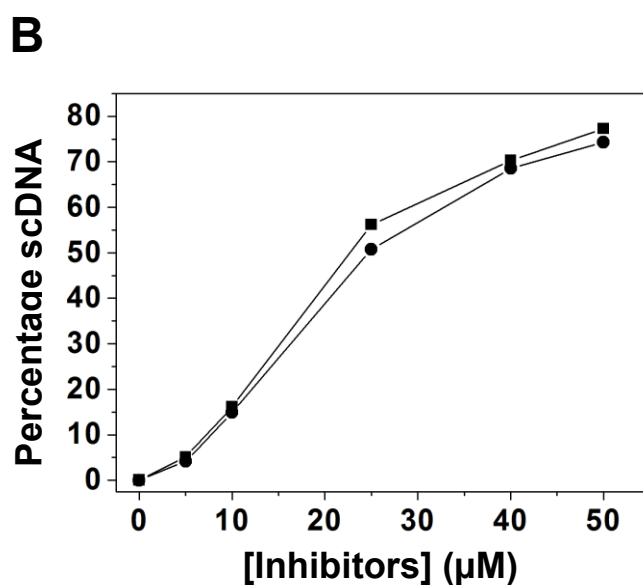
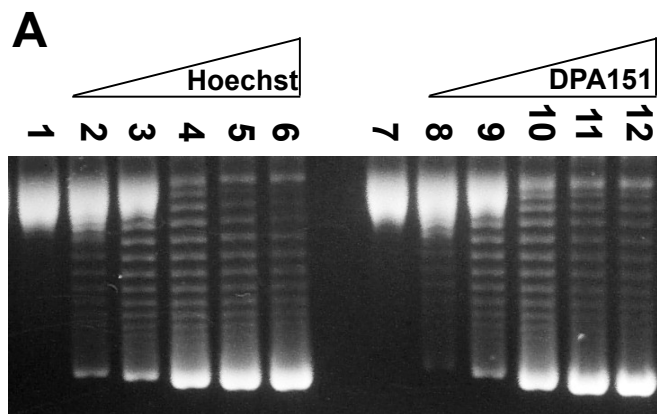


Figure S20. Inhibitory activities of compounds Hoechst 33258 and DPA151 against *human* DNA topoisomerase I. The *human* DNA topoisomerase I inhibition assays were performed as described in Materials and Methods. The plasmid DNA molecules were isolated and subjected to 1% agarose gel electrophoresis in the absence of chloroquine. (A) Lanes 1 to 6 contain 0, 5.0, 10.0, 25.0, 40.0, and 50.0 μM of Hoechst 33258. Lanes 7 to 12 contain 0, 5.0, 10.0, 25.0, 40.0, and 50.0 μM of compound DPA151, respectively. (B) Quantification analysis of the inhibitory activities of Hoechst 33258 (close square) and DPA151 (close circle) against human topoisomerase I.

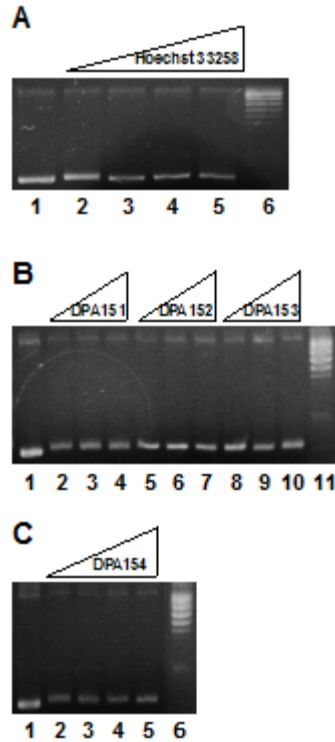


Figure S21. Inhibitory activities of compounds (A) Hoechst 33258, (B) DPA151, DPA152, DPA153 and (C) DPA154, DPA157 against *E.coli* DNA Gyrase. The *E.coli* DNA Gyrase inhibition assays were performed as described in Materials and Methods. The plasmid DNA molecules were isolated and subjected to 1% agarose gel electrophoresis in the absence of chloroquine. (A) Lanes 1 and 6 are the supercoiled and relaxed plasmid DNA pBAD-GFPuv, respectively. Lanes 2 to 5 contain 0, 1.0, 10.0, and 50.0 μM of Hoechst 33258, respectively. (B) Lanes 1 and 11 are the supercoiled and relaxed plasmid DNA pBAD-GFPuv, respectively. Lanes 2 to 4 contain 0, 1.0, and 10.0 μM of DPA151, respectively. Lanes 5 to 7 contain 1.0, 10.0, and 50.0 μM of DPA152, respectively. Lanes 8 to 10 contain 1.0, 10.0, and 50.0 μM of DPA153, respectively. (C) Lanes 1 and 9 are the supercoiled and relaxed plasmid DNA pBAD-GFPuv, respectively. Lanes 2 to 5 contain 0.0, 1.0, 10.0, and 50.0 μM of DPA154, respectively.

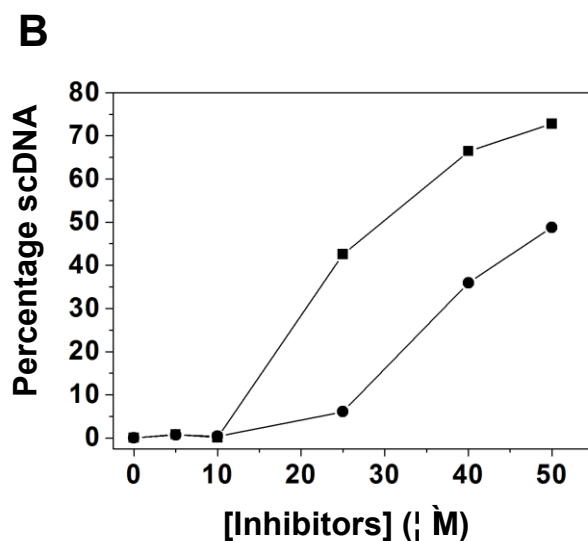
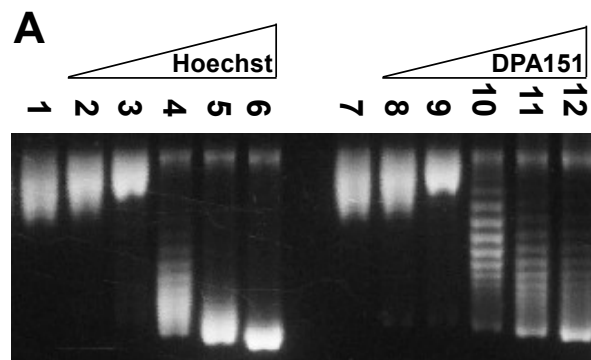


Figure S22. Inhibitory activities of compounds Hoechst 33258 and DPA151 against *human* DNA topoisomerase II. The *human* DNA topoisomerase II inhibition assays were performed as described in Materials and Methods. The plasmid DNA molecules were isolated and subjected to 1% agarose gel electrophoresis in the absence of chloroquine. (A) Lanes 1 to 6 contain 0, 5.0, 10.0, 25.0, 40.0, and 50.0 μM of Hoechst 33258, respectively. Lanes 7 to 12 contain 0, 5.0, 10.0, 25.0, 40.0, and 50.0 μM of DPA151, respectively. (B) Quantification analysis of the inhibitory activities of Hoechst 33258 (close squares) and DPA151 (close circles) against human topoisomerase II.

UV thermal denaturation plots.

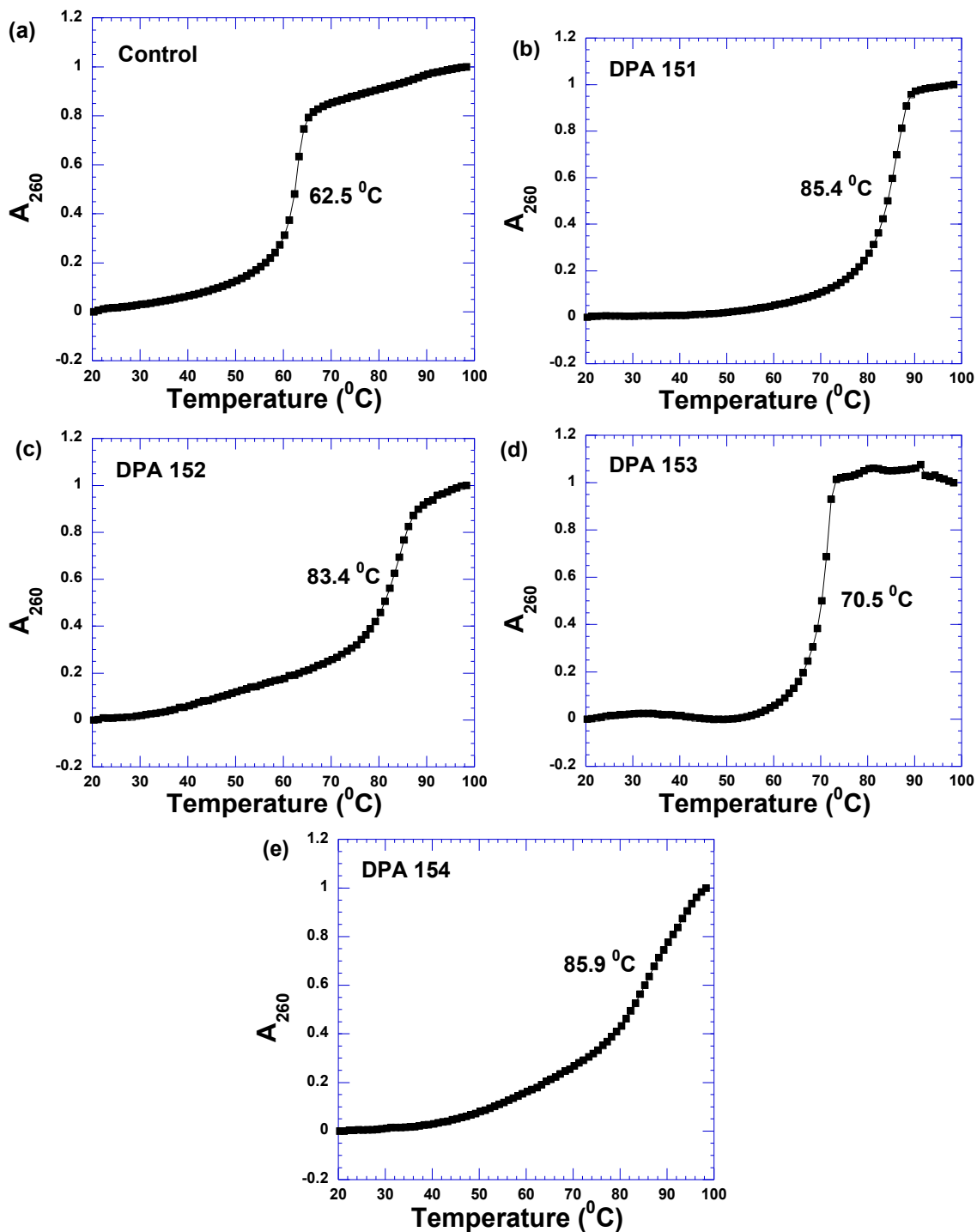
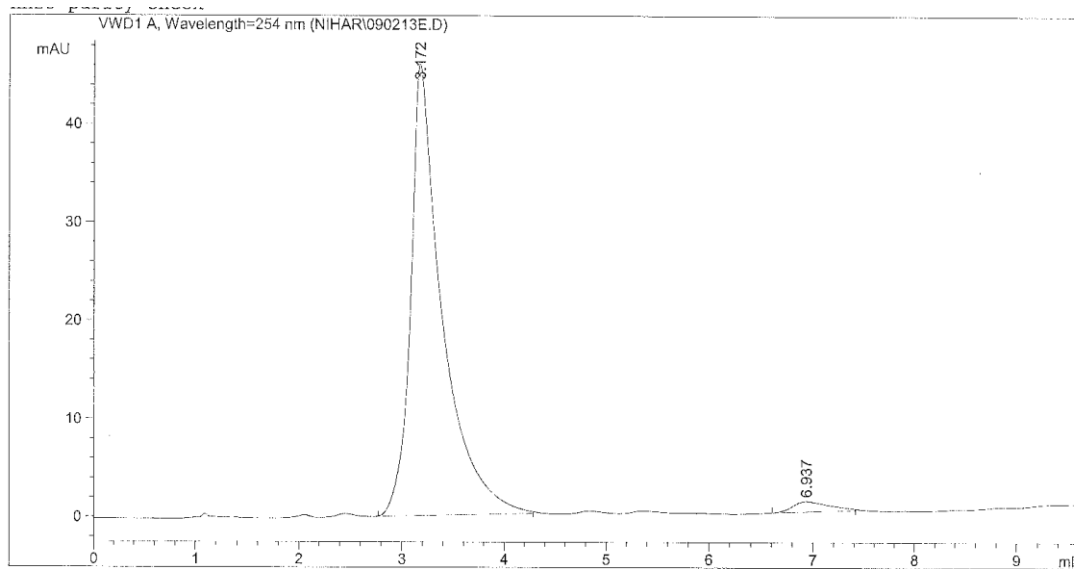


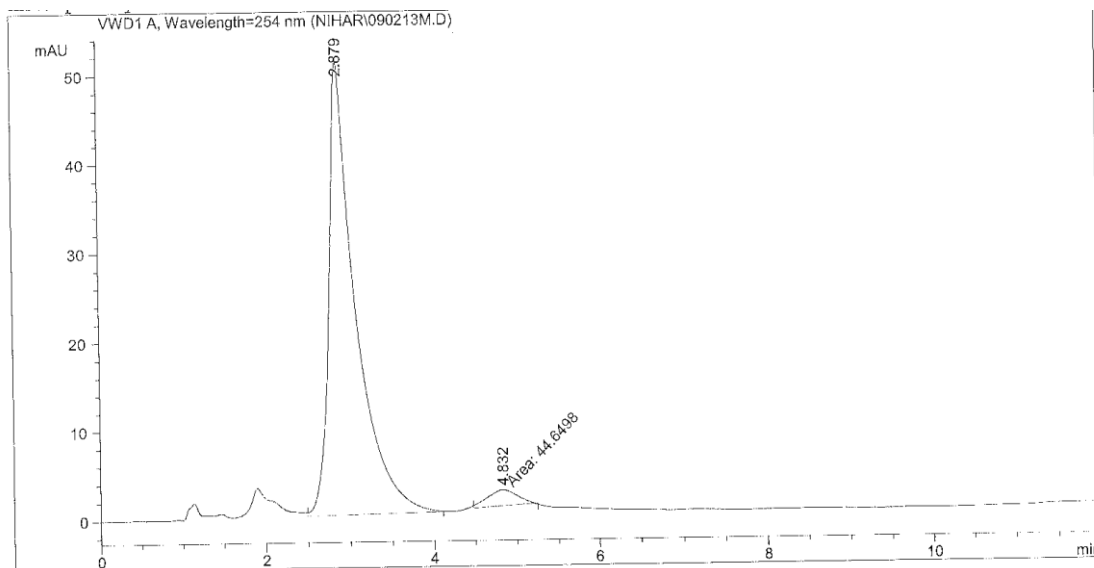
Figure S23. UV thermal denaturation profiles of all ligands studied with $\text{dA}_{60}\text{-dT}_{60}$ duplex. The DNA duplex ($1\ \mu\text{M}$ / duplex) was mixed with various ligands (as indicated on each graph) at $10\ \mu\text{M}$

concentration and denatured in the temperature range 20 °C- 98 °C at a rate of 0.2 °C/min in buffer 10 mM sodium cacodylate, 0.1 mM EDTA and 100 mM NaCl at pH 7.0.

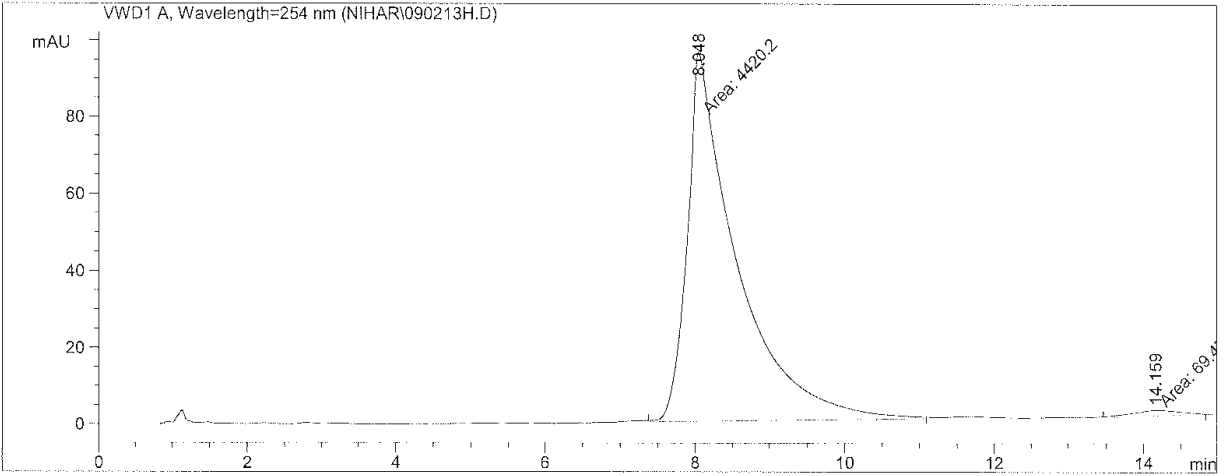
HPLC chromatograms of DPA 151-154.



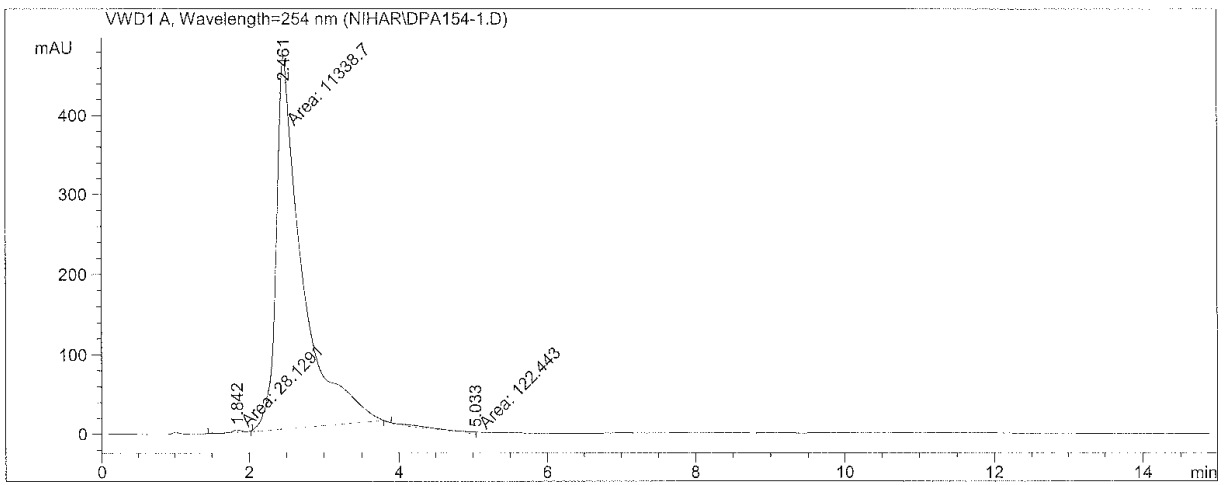
HPLC chromatogram of DPA 151.



HPLC chromatogram of DPA 152.



HPLC chromatogram of DPA 153.



HPLC chromatogram of DPA 154.

Table S1. IC₅₀ values of studies compounds against DU-145.

Ligand	IC₅₀ (μM)
Hoechst 33242	4.25 ± 0.11
DPA 151	3.24 ± 0.71
DPA 152	2.12 ± 0.46
DPA 153	>10
DPA 154	2.79 ± 0.13